People's Democratic Republic of Algeria

Ministry of Higher Education and Scientific Research

University Abbas Laghrour Khenchela

كليـــة العلـــوم والتكنولوجيـــا

قسم الهندسة الصناعية

End of Study Thesis in View of Obtaining the Diploma of Master in Electrical Engineering

Branch : Electrical Control

Subject

Realization of a Solar MPPT Regulator for the Control of a DC-DC Converter

Presented by:

- ✓ **Boukakra Wahiba**
- ✓ **Laasis Nour EL Houda**

Framed by:

- ✓ **Mr: Saidi Abdelkader**

Reviewers :

- ✓ Dr Beddiaf Yassine
- ✓ Mr Labdani Rafik

Academic Year 2020/2021

Acknowledgement

First of all, we thank the good God Almighty who gives us faith, courage and patience during all our years of study.

Thus, we would also like to express our deepest thanks to our supervisor Mr. "Saidi Abdelkader" for having first proposed this theme, for guiding us patiently during all this period. Who did not stop giving us his advice.

Our thanks also go to all the teachers of Electrical Engineering who have contributed to our training, as well as to all the members of the jury who agreed to accepted to judge this modest work.

Finally, we would like to express our gratitude to our families and friends for the moral and material support moral and material support.

Dedication

I dedicate this modest work especially to those who taught me the meaning of life taught me, encouraged me and supported me during my studies, to my father's soul and to my dear mother.

To my great support always my husband ''Sofiane''

To my children ''Roufia, Mohamed, and Yanis ''

To my family and in-laws ,to my father's in law soul

And of course, to my partner Houda.

To my colleagues DJAMEL and Oussama thank you very much.

Wahiba. B

CONTENTS:

List of figures:

Chapter I

List of Figures

Chapter II

Chapter III

List of Figures

Chapter IV

List of Figures

List of tables:

CHAPTER I

CHAPTER III

CHAPTER IV

List of abbreviations:

I:	Cell current [A]
Iph:	The photo-current [A]
Ish :	The current flowing through the shunt resistor [A]
Irs :	Diode saturation current [A]
Vd :	Voltage across the diode [V]
T:	Cell temperature [K]
n:	Ideality factor of the diode
T:	Cell temperature [K]
G:	Irradiation [W / m ^ 2]
Gref :	The reference irradiation = 1000 [W / m ^2]
Tref :	The reference temperature = 25 ° C = 298 K
Isc :	The short-circuit current of the cell [A].
Ipv :	Current of the GPV [A]
Vpv :	GPV voltage [V]
Ns:	Number of cells connected in series per module
N_p :	Number of modules connected in parallel.
L:	Represents the inductance [H].
Id:	Diode current (A)
Vd :	Diode voltage (V)
Io:	Diode saturation current (A)
T:	Cell temperature (K)
Ncell:	Number of cells connected in series in solar panel
AC:	Alternating current
DC:	Direct current
Vo:	Voltage at the terminals of the load

S: Switch

IL : Inductance current

Vi : Input voltage

SC: Static converter

HC: Hill climbing

P&O: Perturb and Observe

MPPT: Maximum power point tracking

PV: photovoltaic generator

MPP: Maximum Power

Point Isc: Short circuit current

Voc : Open circuit voltage

D: Duty cycle

PV: Photovoltaic

Vpv: PV voltage

Ipv: PV current

Ppv: PV power

i: iteration

Eff: efficiency

ΔP: variation of the power

ΔI: variation of the current

dG: variation (increment) of conductance

ΔD: change of the duty cycle

General Introduction

General introduction:

Solar energy is a promising source of energy for the near future. PV modules are connected in series and parallel manner so as to collect and harness the solar energy obtained convert it into electrical energy.

Generically stating, an independent PV system consists of PV arrays which convert sunlight into DC electricity. In addition, it also includes a charge controller to regulate the battery charging and discharging.

A charge controller is one of the major functional components in PV systems which maintains the accurate charging voltage on the batteries. As solar energy is not evenly distributed, research is being done on various methods of collection such as thin-film devices, concentric collectors etc. [1].

DC-DC converters are power electronics circuits. They are widely used in equipment to supply power to many electronic instruments such as PCs, and also in specialized high power applications such as battery charging, etching, soldering, etc. In addition to control and step-down and/or step-up DC voltage transformation, DC-DC converter circuits can also generate voltage isolation through a small high frequency transformer. [2].

The wide variety of DC-DC converter circuit topologies range from simple switches (Buck, Boost, and Buck-Boost converters) to complex configurations with two to four switches and employing simple switching or resonance techniques to control the step-down or step-up switching. [3].

The objective of our current work is to harness electrical power generation from a photovoltaic generator by from a photovoltaic generator by implementing a measurement chain for the electrical components of the of the power. This digital acquisition will be exploited by an embedded platform (e.g. arduino) to implement a maximum power point search algorithm MPPT. In this thesis, we analyze the modelling and simulation of the electrical operation of a photovoltaic system adapted by three controls (MPPT control: perturbation and observation, hill climbing, incremental conductance) ensuring the tracking of the maximum power supplied by the photovoltaic generator. The objective of this work is to study a better understanding of the performance of the MPPT-adapted DC-DC converter when coupled to a photovoltaic array and to improve its output voltage in order to obtain a good source that can be used as a power generator. To describe this, this thesis is presented in four chapters:

In the first chapter, we will describe the most used solar cells and their operating principles, as well as the modeling of a photovoltaic cell and the influence of different meteorological

parameters (temperature and irradiation). Towards the end of this chapter, we will present the photovoltaic system and mention some advantages of the latter.

In the Second chapter, three types of DC-DC converters, among the most commonly used in photovoltaic systems for source-to-load matching, are presented. Therefore, it is necessary to use a technique that ensures the conversion of the maximum power from the solar panel to the load by performing a search for the MPP. This search is done by combining a DC-DC converter between the solar panel and the load.

The Third chapter is devoted to the study of various selected MPPT algorithms by grouping them according to their principles. The most commonly encountered are: Hill climbing, Perturb and Observe and Incremental Conductance Then Implementing those techniques in the psim software.

The Fourth chapter contains two parts the first is about the simulation of the PV system adapted with the buck converter and controlled with the MPPT regulator using proteus version 8.11 and the second part is about the realization of the Mppt regulator using the perturb and observe technique at the electronics lab.

At the end, we conclude this thesis with a general conclusion.

CHAPTER I :

General Information on Phtovoltaic Systems

I.1 Introduction:

Solar photovoltaic energy is energy that is recovered and converted directly into electricity from sunlight by photovoltaic panels. It results from the direct conversion of a photon into an electron in a semiconductor.

Photovoltaic solar energy is a non-polluting source of energy and is available in abundance all over the Earth's surface, and despite significant attenuation when it passes through the atmosphere, the amount that remains is still quite significant when it reaches the ground. In temperate zones, 1000 W/m² peak can be expected, and up to 1400 W/m² when the atmosphere is lightly polluted.

This chapter describes the functioning of solar photovoltaic energy and gives the theoretical basis of the different components of a photovoltaic system and the types of installations of photovoltaic systems. [4].

Figure I.1: photovoltaic energy.

I.2 Photovoltaic solar energy:

Refers to the energy recovered and transformed directly into electricity from sunlight by photovoltaic solar panels. It results from the direct conversion of photons into electrons in a Semi-conducteur (Silicon, CdTe, AsGa, CIS, etc.).

FigureI.2: Solar Photovoltaic Plant.

I.2.1 Photovoltaic effect:

The photovoltaic effect is a physical phenomenon specific to certain materials called "semiconductors". This physical phenomenon occurs when the surface of a cell is exposed to light, an incident photon (light grain) interacts with the electrons of the material, it gives up its energy to the electron, which is freed from its valence band and is therefore subjected to the intrinsic electric field. Under the effect of this field, the electron migrates towards the upper surface, leaving a hole which migrates in the opposite direction. Electrodes placed on the upper and lower faces allow the electrons to be collected and to perform electrical work to join the hole on the front face. [5].

I.2.2 Elements of a photovoltaic system:

In general, a photovoltaic system consists of a set of photovoltaic modules, a charge controller, one or more batteries and an inverter (Figure 1.3).

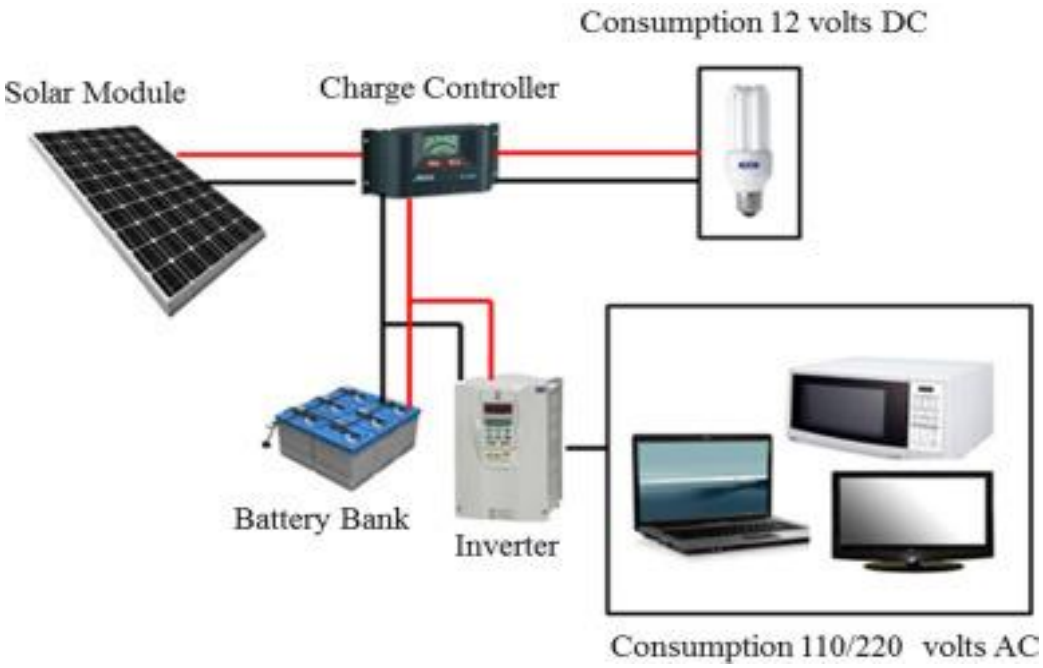

Figure I.3: Block diagram of a photovoltaic system.

The photovoltaic generator (GPV) represents the electrical energy production part.The regulator is an electronic circuit whose role is to manage the flow of current: current from the panels to charge the battery and current from the battery to the consumers. It manages the charging and discharging of the battery by disconnecting the panel when the batteries are charged or by cutting off the supply to the consumers when the battery is too discharged.

Batteries are used for energy storage for direct use of direct current (DC) with a DC load.In the case of alternating current (AC) use, the DC energy will be converted into AC energy through an inverter. [5].

I.2.3 Photovoltaic generator:

A PV generator is defined by the whole assembly of solar cells, connections, protective parts and supports, etc. The term "PV generator" can therefore be represented by any PV device (solar cells, modules, panels...).

a) Photovoltaic module:

A photovoltaic module consists of several solar cells connected to each other (Figure 1.4). Generally, each photovoltaic cell can only produce a nominal DC voltage of 0.5V to 0.6V in open circuit and a nominal power of about 1.5Wp. To meet the needs of commonly used loads, an assembly of several photovoltaic cells must be considered, either in series or in parallel. This assembly forms what is called a "solar module" or "photovoltaic module".

The dimensioning of the solar system determines the number of modules to be put either in parallel in order to increase the current while keeping the voltage or in series in order to increase the voltage while keeping the current, and to have a satisfaction in current and voltage, a mixed grouping "series-parallel" is mandatory. [5].

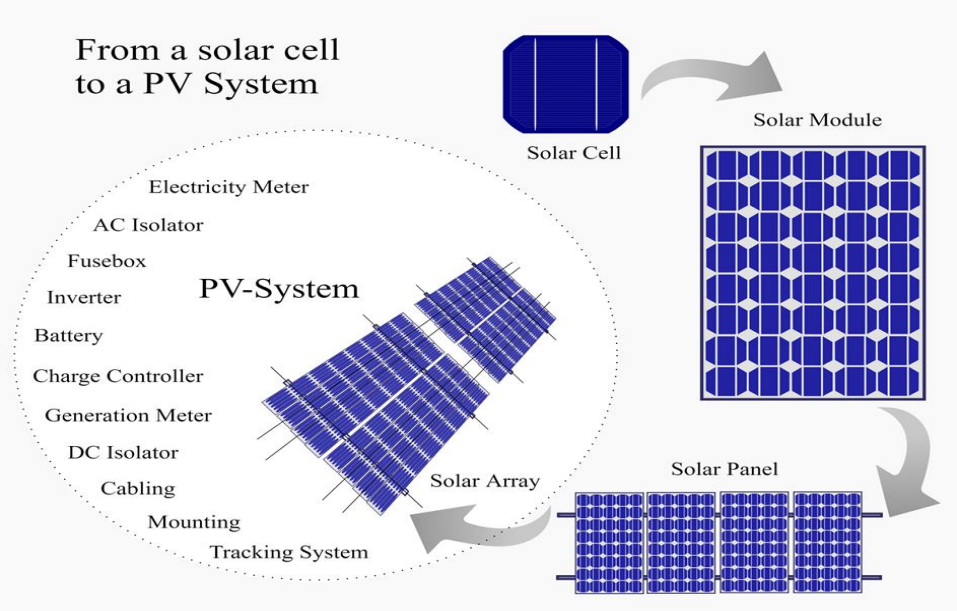

***Figure I.4: from* a solar cell to a PV system.**

b) Composition of a solar photovoltaic module:

A solar photovoltaic module generally consists of five components (Figure 1.5):

- Aluminum frame: aluminum is infinitely recyclable.
- Tempered glass: is a 100% recyclable material, used for the protection of the module and represents 75% of the composition of the panel.
- Transparent EVA sheet (EVA: Ethylene Vinyl Acetate): to resist weathering and moisture.
- Photovoltaic cells: this is the electronic component that produces electricity, mainly based on silicon, and can be reused up to 4 times.
- White Tedlar sheet: for greater mechanical strength of large modules.

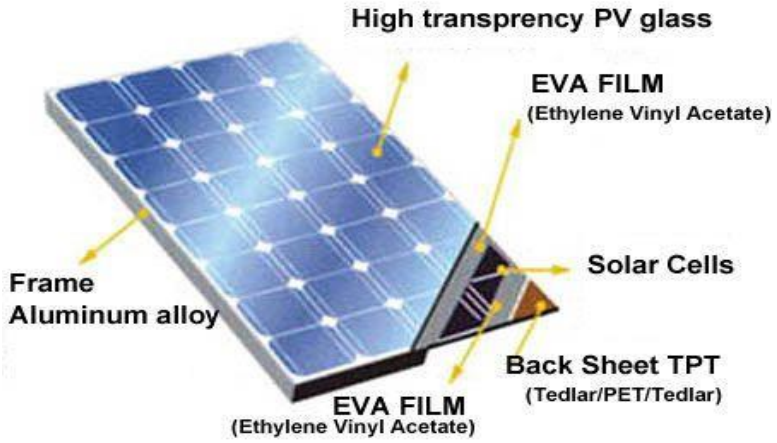

Figure I.5: Composition of a solar photovoltaic module.

In order to ensure a long lifetime of a photovoltaic installation intended to produce electrical energy over many years, electrical protections must be added to commercial modules to avoid destructive failures due to the combination of cells in series and panels in parallel. For this purpose, two types of conventional protections are used in current installations (Figure I.6).

c) Photovoltaic parameters:

A PV module is the smallest set of interconnected solar cells. There are many parameters that characterize a PV module, including

- **Maximum power (Pm): this is** the maximum electrical power that the module can deliver under standard conditions (T = 25°C and 1000 W/m² illuminance).
- **Open circuit voltage (Voc): this is** the voltage across the module when not connected to a load for "full sun" illumination.
- **Short circuit current (Isc)**: current when the potential applied to the module is zero. This is the highest current the module can deliver, for "full sun" illumination.
- **Optimum operating point (Vm, Im):** when the power is at its maximum in full sunlight, $Pm = Vm.\ Im$.

The I/V characteristic: curve representing the current (I) delivered by the module as a function of the voltage (V) at its terminals. [5].

d) Photovoltaic cell:

The PV cell is the smallest element of a photovoltaic system. It is made of semiconductor material and is made of two layers, one doped with P (Positive, doped with Boron for example), and the other doped with N (Negative, doped with Phosphorus for example). This creates a PN junction, and directly transforms light energy into electrical energy. A cell consists of a stack of layers: protective glass, anti-reflection layer, conductive mesh (cathode), N-doped silicon, NP junction, P-doped silicon and a metal support (anode), as shown in the following figure: [6].

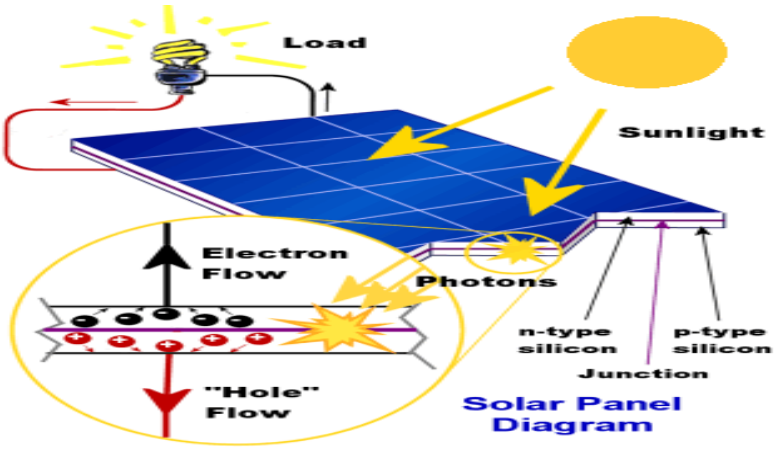

Figure I.6: Components of a solar cell.

e) The Different Types of Photovoltaic Cells:

Photovoltaic cells are made of semiconductors based on silicon (Si), germanium (Ge), selenium (Se), cadmium sulphone (CdS), cadmium telluride (CdTe) or gallium arsenide (GaAs). Silicon is currently the most common material used to make photovoltaic cells, as it is very abundant in nature. It is found in nature in the form of silica stone. Silica is a chemical compound (silicon dioxide) and a mineral with the formula SiO2. It is the main constituent of detrital sedimentary rocks (sands, sandstones). [6].

The different types of PV cells available are:

- Amorphous silicon cell (efficiency: 6 to 10%)
- Monocrystalline silicon cell (efficiency: 13 to 17%) Polycrystalline silicon cell
- (Efficiency: 11 to 15%) Tandem cell
- Organic cell (efficiency: 3.6%).

Table I.1 different types of photovoltaic cells

Monocristalline Cells :	Polycristalline Cells	Amorphous Cells
each layer is cut from a silicon single crystal. This type of cell has very good efficiency and converting power, but is very expensive.	they are also very efficient cells, but slightly lower than that of Monocrystalline cells, which justifies their lower cost.	this type of cells do not have crystal structures. They have the advantage of being integrated on flexible and rigid supports. They are often used in portable devices, calculators, watches, etc.
		

f) Association of photovoltaic cells:

There are three types of PV cell combinations:

- **Association in series: [7].**

The combination of cells in series (figure I.7) allows the voltage (the sum of the voltages) to be increased while maintaining the current of one cell.

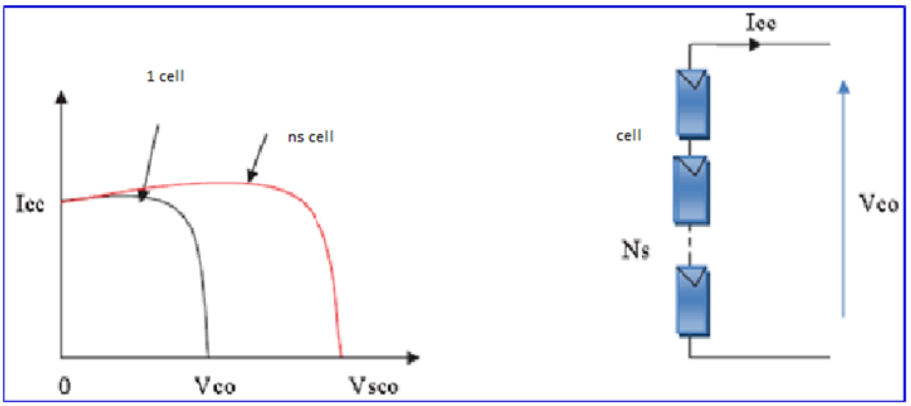

Figure I.7: Association of ns PV cells in series and the current-voltage characteristic of ns cells in series.

- **Parallel association :**

The combination of cells in parallel (figure 1.8) allows the current (the sum of the currents) to be increased while maintaining the voltage of a cell.

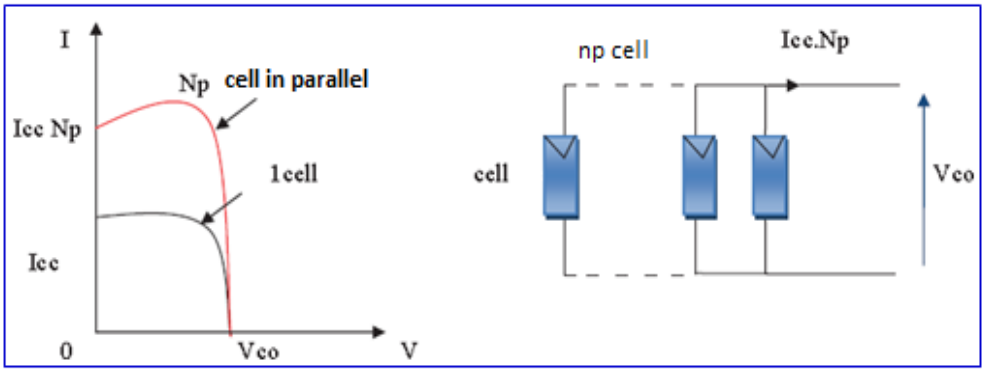

Figure I.8: Association of np cells in parallel And The I(V) characteristics.

- **Mixed association (serial-parallel) :**

The mixed combination (Figure 1.10) is based on connecting the cells in series and in parallel, which allows the current and voltage to be increased at the same time.

The I(V) characteristic of a solar module can be seen as the result of an association of an array of ($ns*np$) cells in series/parallel.

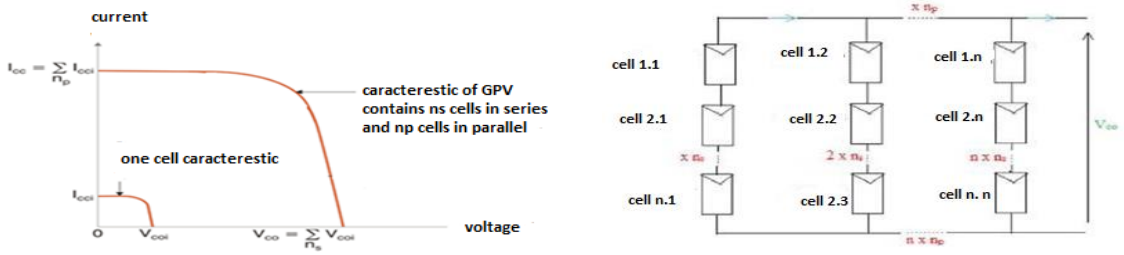

Figure I.9: Mixed cell association (serial-parallel) and the characteristic of a serial/parallel assembly of ns and np cells.

- **Parallel diode protection (by-pass diode):** aims to protect a series of cells in the event of an imbalance linked to the failure of one or more of the cells in the series or to shading on certain cells.
- **The series diode (anti-return diode):** placed between the module and the battery, prevents the return of current to the module during darkness.

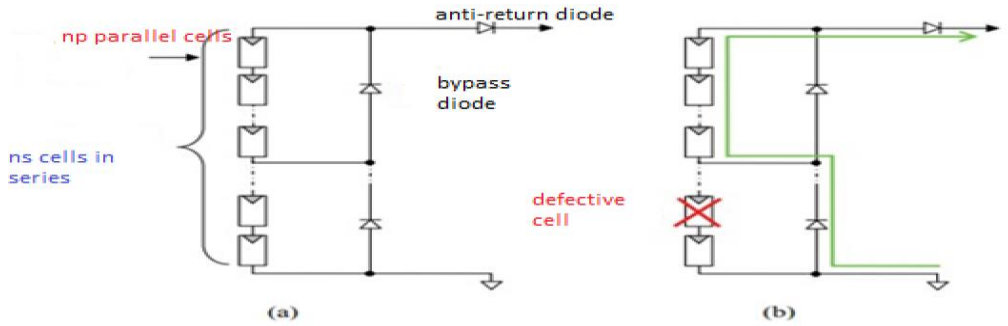

Figure I.10: (a) Schematic of a photovoltaic solar panel with protection diodes (b) Failure of one of the cells in the PV module and activation of the bypass diode and demonstration of the circulation current.

g) Electrical characteristics of a photovoltaic cell:

There are many parameters that can be used to characterize a solar cell. These parameters are called photovoltaic parameters and are derived from the I(V) and P(V) characteristic. Figure (1.11) shows an example of a current-voltage I(V) and power-voltage P(V) characteristic for a given irradiance and temperature. **[7].**

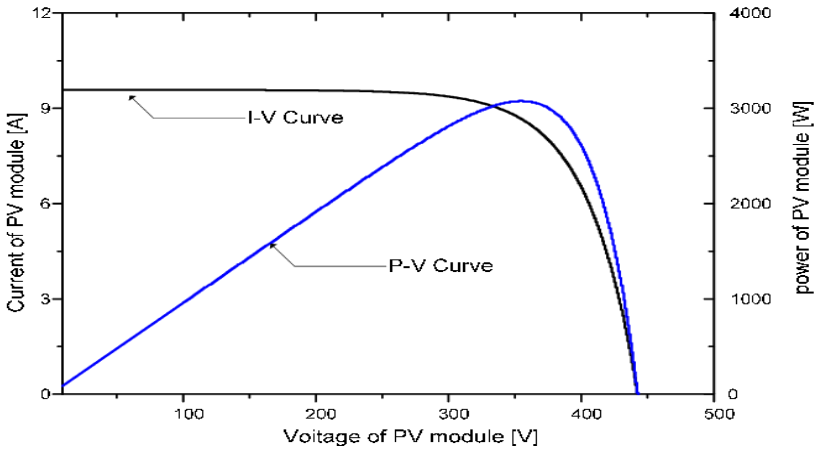

Figure I.11: Characteristic I (V) and P (V) for (G=1000 W/m2 and T=25°c) of a Cell.

➢ Influence of température : [8].

Below we present the (*I-V)* and (*P-V)* characteristics (Figure 1.13and 1.14) of a photovoltaic module for a given level of sunlight G and for different temperatures:

For figure (1.**12**), we notice that the current depends on the temperature since the current increases slightly as the temperature increases; we can see that the temperature has a negative influence on the open circuit voltage. When the temperature increases the open circuit voltage

decreases. And on the other hand the maximum power of the generator undergoes a decrease when the temperature increases figure (1.**13**).

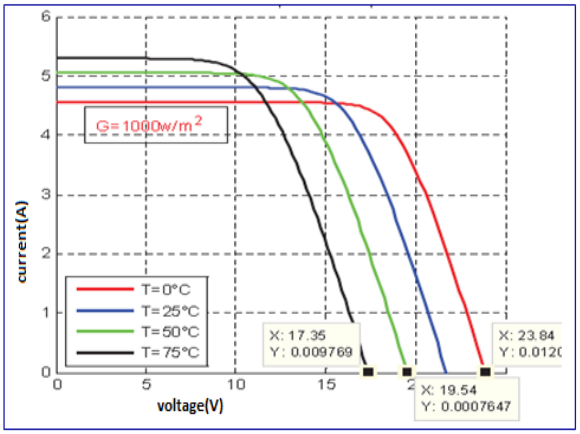

Figure I .12: The characteristic of I=f (V) As a function of temperature

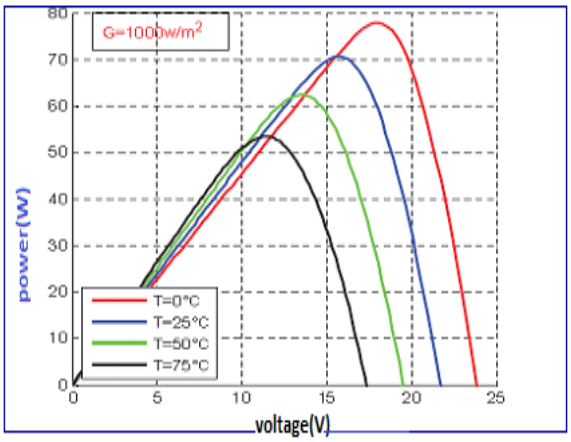

Figure I.13: The characteristic of P= f (V) as a function of temperature

➢ Influence of irradiation: [8].

The same work as before, we have fixed the temperature for different illuminations figure (1.14 and 1.15). In figure (1.14) it can be seen that for illumination G=1000 w/m2 the current *Icc=4*.8A and for G=800w/m2 the current *Icc=3*.84A, it can be seen that the current undergoes a significant variation, when the illumination increases the short circuit current is increased, but on the other hand the voltage varies slightly, which results in an increase in power, when the illumination is increased figure (1.15).

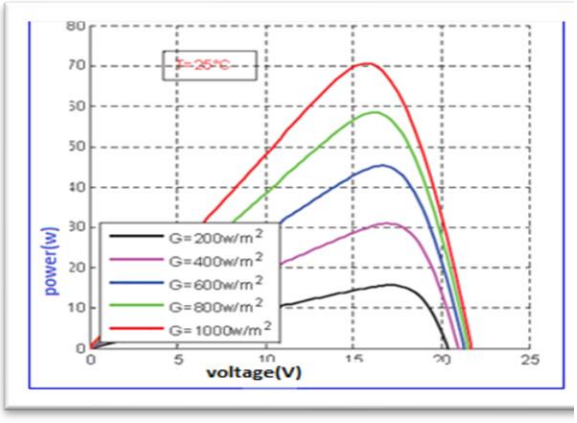

Figure I.14: The I=f (v) characteristic as a function of irradiation

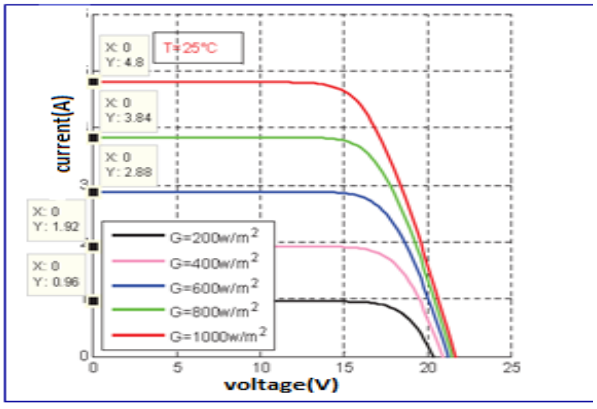

Figure I .15: The characteristic P=f(v) as a function of irradiation

I.2.4 Different models of the GPV: [9].

a) Simplified model:

The principle of the photovoltaic effect is the same as that of a diode, so when the PN junction is illuminated, the cell being loaded by a resistor, we observe the appearance of a current "I" passing through it junction, the cell being loaded by a resistor, we observe the appearance of a current "I" crossing a load .Rch and a voltage ‘‘V’’. a load Rch, and a voltage "V" at the terminal of this load.

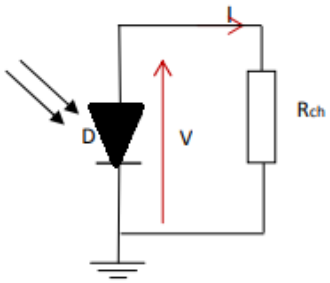

Figure I.16: Application diagram of the photovoltaic effect.

b) IDEAL MODEL:

The previous reflection allows us to arrive at the equivalent electrical model of the photovoltaic cell shown in Figure 1.18, called the ideal model.

photovoltaic cell shown in Figure 1.18, called the ideal model. This is the simplest model to represent the solar cell, as it only takes into the account This is the simplest model to represent the solar cell, as it only takes into account the diffusion phenomenon. The simplified equivalent circuit of a solar cell consists of a diode and a current source connected in parallel . The current source produces the photon current Iph which is directly proportional to the solar irradiance G.

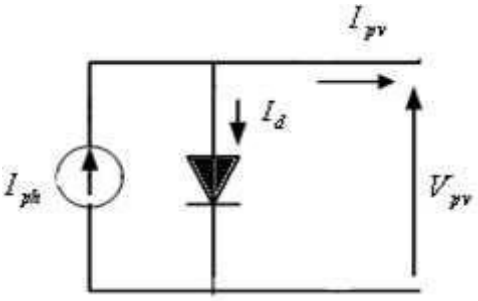

Figure I.17: Equivalent circuit of a PV cell -ideal model.

The current-voltage equation I-V of the equivalent circuit is given as follows:

$$I = I_{PV} - I_d \qquad (I.1)$$

With:

I: current supplied by the cell

I_{PV}:Photon-current of the cell proportional to the luminance (G)

$$\boldsymbol{I_D = I_0\left[\exp\left(\frac{V}{aV_T}\right) - 1\right]\ avec : V_T = \frac{k \cdot T}{q}} \qquad (I.2)$$

Thus the equation for the current delivered by a photovoltaic cell is described as follows:

$$I = I_{PV} - I_0\left[\exp\left(\frac{V}{aV_T}\right) - 1\right] \qquad (I.3)$$

With:

I_0: reverse saturation current of the diode.

V_T: Thermodynamic potential.

K: Boltzmann's constant (1.38.10-23 Joules/Kelvin).

T: The cell temperature in Kelvin.

q: The charge of an electron =1.6.10-19C.

a: The ideality factor of the junction.

v: The terminal voltage of the cell

c) MODEL WITH OHMIC LOSSES (Rs-MODEL):

This model takes into account the resistivity of the material and the ohmic losses due to the contact levels, which allows a better representation of the electrical behavior of the cell compared to the ideal model [10,11]. These parts are represented by a series resistance Rs in the equivalent circuit shown below:

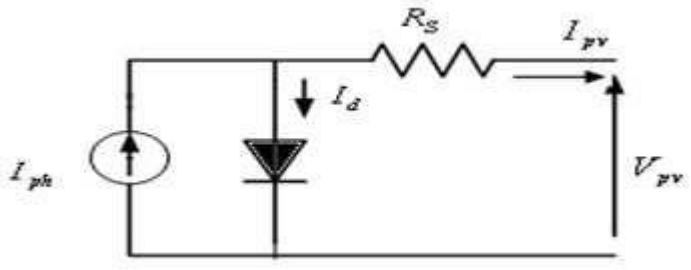

Figure I.18: PV cell equivalent circuit -Rs-Model -

After analysis of the circuit, the current-voltage equation is given as follows:

$$I = I_{PV} - I_0\left[e\left(\frac{V+IR_s}{aV_T}\right) - 1\right] \qquad (I.4)$$

With:

R_S: The series resistance characterizing the various contact and connection resistances.

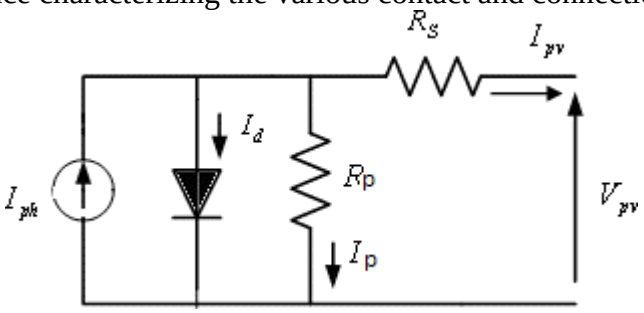

Figure I.19: Equivalent circuit of a PV cell - 1-D model.

The equation of the current delivered by the photovoltaic cell is described as follows:

$$Ipv = Iph - Id - Ip \quad (I.5)$$

Ipv: Current generated by the photovoltaic cell

Iph: Photo current created by the cell (proportional to the incident radiation)

Id: The current flowing in the diode.

$$I_d = I_0(e^{-\frac{V_d}{V_t}} - 1) \quad (I.6)$$

$$Vpv = V_d - R_s Ipv \quad (I.7)$$

$$I_p = \frac{V_d}{R_p} \quad (I.8)$$

ISC: The short circuit current of the cell at the reference temperature and illumination;

T: PV cell junction temperature [°K]

B: Ideality factor of the junction

Eg: Gap energy [ev].

Rs: Series resistance symbolizes the ground resistance of the semi-conductor material, thus the ohmic and contact resistances at the cell connections.

Vpv: The output voltage

Ip : Current flowing through the resistor RP

Rp: The resistance modelling the leakage currents of the junction.

$$\mathrm{Ipv} = I_{ph} - I_0\left[\mathrm{e}^{-\frac{\mathrm{Vpv}+R_s\mathrm{I}}{V_t}} - 1\right] - \frac{\mathrm{Vpv}+R_s\mathrm{I}}{R_p} \quad \text{(I.8)}$$

$$Ip = \frac{\mathrm{Vpv}+R_s\mathrm{I}}{R_p} \quad \text{(I.9)}$$

d) TWO DIODS MODEL:

This model is said to be the closest to the real behavior of the solar cell, because it takes into account the mechanism of charge transfer inside the cell, the additional diode allows to reproduce in the additional diode allows the chemical effects of electron recombination to be reproduced in the equivalent scheme [9].

Single diode models have been based on the assumption that the recombination loss in the depletion region is absent. In a real solar cell, recombination represents a considerable loss, which cannot be adequately loss, which cannot be adequately modeled using a single diode. Examination of this loss leads to a more accurate model known as the two-diode model. However, the inclusion of the diode increases the parameters to seven (new parameters: I02, F2. The main challenge is now to the main challenge now is to estimate the values of all model parameters, while maintaining a reasonable computational effort.

The two-diode model is presented as follows:

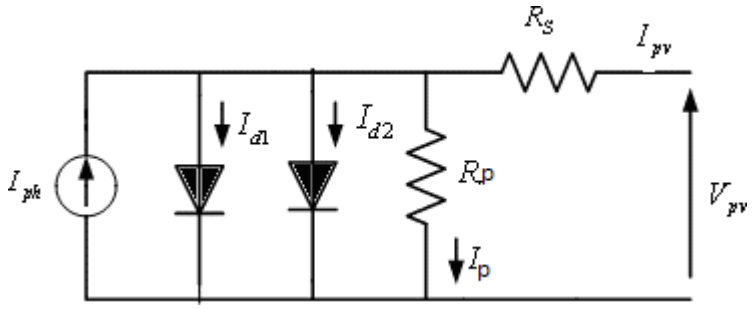

Figure I.20: Equivalent electrical diagram of a crystalline silicon cell - 2-DRs model

The following equation describes the output current of the photovoltaic cell for the two-diode model:

$$\mathrm{I} = \mathrm{I_{PV}} - \mathrm{I_{01}}\left[\exp\left(\frac{\mathrm{V}+\mathrm{IR_s}}{\mathrm{a_1 V_{T1}}}\right) - 1\right] - \mathrm{I_{02}}\left[\exp\left(\frac{\mathrm{V}+\mathrm{IR_s}}{\mathrm{a_2 V_{T2}}}\right) - 1\right] - \left(\frac{\mathrm{V}+\mathrm{IR_S}}{\mathrm{R_p}}\right) \quad \text{(I.10)}$$

With:

I_{01}: reverse saturation current of diode D1.

I_{02}: Reverse saturation current of diode D2.

V_{T1}: Thermodynamic potential of diode D1.

V_{T2}: Thermodynamic potential of diode D2.

a_1: The ideality factor of the junction of diodeD1.

a_2: The ideality factor of the diodeD2 junction.

e) OTHER MODELS:

Many authors have proposed more sophisticated models that represent more accurately the photovoltaic phenomenon. the photovoltaic phenomenon. We thus find the three-diode model, with the third diode including in the equivalent diagram the effects not taken into account in the other models (e.g., leakage current due to diodes).

leakage currents related to the diodes). The disadvantage of this representation is that the number of unknown parameters.

The disadvantage of this representation is that the number of unknown parameters increases as the number of diodes in the schematic increases.

On the other hand, more simplified models are also emerging: the value of the resistance Rp

The value of the resistance Rp is generally high, so it is often assumed to be infinite and therefore neglected in the current models.

The value of the resistance Rp is generally high, so it is often assumed to be infinite and therefore neglected in the current models, and the value of the resistance Rs is generally low, so the authors of equivalent models often assume Rs=0 and

equivalent models often assume Rs=0 and therefore neglect Rs, so that we return to the equivalent circuit of the ideal model. But, unfortunately, this model loses accuracy.

I.2.3 Identification of the parameters of the photovoltaic module: [9].

It is well known that the parameter identification step of any system is a very important step for both simulation and practice. Therefore, as for any system, an accurate knowledge of the photovoltaic module parameters is essential for simulation, quality control and performance estimation.

Photovoltaic cell and panel manufacturers usually provide a data sheet containing some parameters of the photovoltaic panel consisting of a group of several cells. But there are other parameters that are not provided on the data sheet. In practice, the determination of these unknown parameters is very important. In this section, one of the important issues related to photovoltaic systems is the determination of these unknown parameters.

The main objective is to find the five parameters of the nonlinear I(V) equation from the data obtained from the PV module data sheet. In order to identify the parameters of the PV panel, we performed our experiments on a 100 W solar panel, and another one of 5 W with the characteristics listed in the tables:

Table I.2 Specifications of the PV module 100W

Maximum power, P_{max}	100W
voltage at P_{max} ,V_{mp}	18.35V
Current at P_{max} , I_{mp}	5.45A
Short- circuit current, I_{sc}	5.8A
Open-circuit voltage, V_{oc}	22.7V

Table I .3: Specifications of the PV module 5W

Maximum power, P_{max}	5W
voltage at P_{max} ,V_{mp}	9 V
Current at P_{max} , I_{mp}	0.56 A
Short- circuit current, I_{sc}	0.62 A
Open-circuit voltage, V_{oc}	11.1V

I. 3 source coupling: [10].

I. 3 .1 Direct source-load coupling:

he simplest PV installation that can be designed consists of a photovoltaic field, formed by one or more modules connected in series or in parallel, and a DC load that directly uses the energy produced.

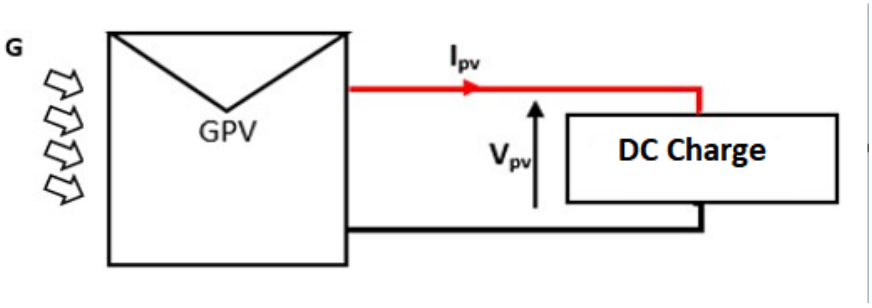

Figure I.21: direct coupling between a GPV and a resistive load

In this type of installation, this is today the most widespread terrestrial use of solar energy thanks to its simplicity, reliability and low cost, the operating point of the GPV depends on the impedance of the load to which it is connected. of the GPV depends on As shown in figure 1.22, a GPV can be directly connected to three types of loads:

- a DC voltage source type load,
- a DC current source load,
- a purely resistive load.

I. 3 .2 indirect coupling:

So the main disadvantage of this installation is that it does not offer any type of operating control. The transfer of the optimal power available at the GPV terminals to the load is not guaranteed either. On the other hand, some types of loads require alternating voltages and currents.

To solve this problem and to extract, at each moment, the maximum power available at the terminals of the GPV and to transfer it to the load, a matching stage is used. This stage acts as an interface between the two elements, figure (1.23). It ensures, through a control action, the transfer of the maximum power supplied by the generator [10].

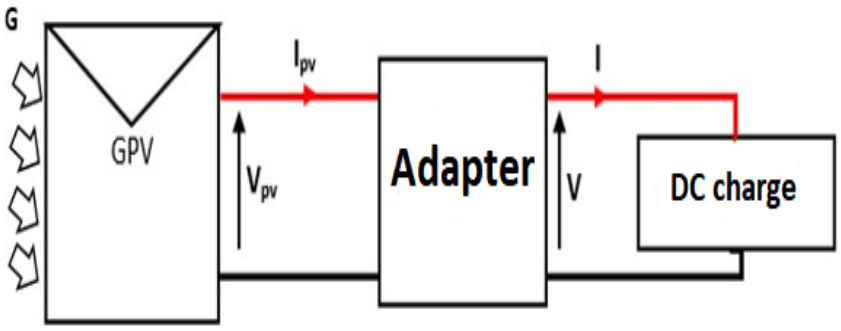

Figure I.22: Connection of a GPV to a DC load through an Adapter.

I.4 Conclusion:

In this chapter we have presented the solar energy and its radiation, following the principle of the photovoltaic effect and the PV cell, as well as the photovoltaic generator,

we have studied the influence of illuminance and temperature on the power produced by the GPV. Finally, the problem of direct source-charge coupling and their solution (the adaptation stage).

In the following chapter, we will present a study on the components of the adaptation stage and their modeling by the PSIM software.

CHAPTER II :

Static Converters

II.1 Introduction:

A static converter is a system that adapts the source of electrical energy to a given receiver by it. The first electrical power converters were made with mechanically coupled electrical machines. With the advent of semiconductors and power electronics, with diodes, transistors, thyristors, etc., conversion systems are becoming more and more sophisticated and no longer require rotating machines. This is the era of the static converter.

There are several families of static converters:

Continuous ⟶ Continuous (Chopper)

Continuous ⟶ Alternating (Inverter)

Alternating ⟶ Alternating (Dimmer)

Alternating ⟶ Continuing (Rectifier)

Conventionally, grid-connected photovoltaic conversion systems consist of DC-DC converter and Inverter (DC-AC). The DC-DC converter is controlled for the maximum power point control system of the photovoltaic panel. The inverter is controlled to produce current in such a way that the current has a low total harmonic distortion and is in phase with the grid voltage **[22].** The aim of this chapter is the presentation and study of the different definitions and basic concepts of DC-DC converters, as well as the mathematical models useful to study their behavior when simulating the overall photovoltaic system **[12].**

II.2 Static converters:

Static converters are electrical circuits using power semiconductors (diodes, thyristors, transistors ...) used as switches, with the aim of transforming the signal spectrum (amplitudes, frequencies, phases) to adapt the source to the load. The study and design of these devices is often called power electronics [13].

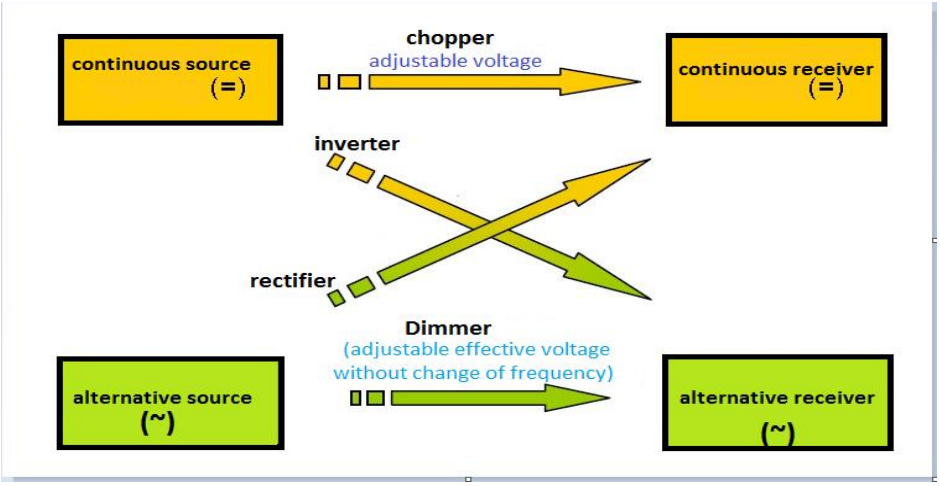

Figure II.1: synoptic diagram of different types of static converters.

The following converters can be distinguished:

II.2.1 the rectifiers:

A rectifier, also known as an AC/DC converter or Graetz bridge, is a converter designed to supply a load that needs to be supplied with a voltage and a current that are both as continuous as possible, from an AC voltage source. The power supply is usually a voltage generator. Non-controlled rectifiers, mainly made from diodes, are used when the output voltage does not need to be adjusted. Controlled rectifiers, where the output voltage can be varied, are made of thyristors or diode and thyristors combinations. Due to their high-power density, these rectifiers are always used at high power levels and when it is necessary to regulate or vary the electrical output values.

At low and medium power levels, thyristors-controlled rectifiers are becoming obsolete and are advantageously replaced by the "cascading" of a controlled or uncontrolled rectifier and a DC-DC Converter. At low power levels.

the control of a field effect transistor or an IGBT is simpler than that of a thyristor. Furthermore, the operating frequencies of choppers, which are now in the 200 kHz range, make it possible to considerably reduce the size of the filtering components (inductors and capacitors). Finally, there are sinusoidal absorption rectifiers built with diodes, ballast MOSFETs or IGBTs which are used to improve the waveform of the AC current consumed on the grid side. [14].

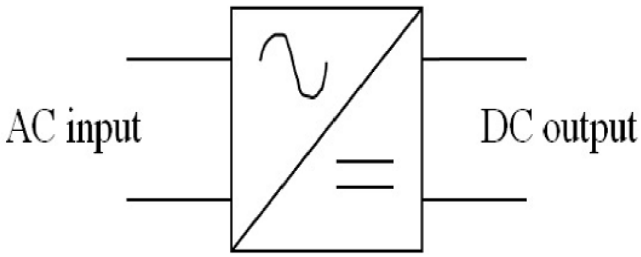

Figure II.2: the rectifier synoptic diagram.

II.2.2 Inverters:

A power inverter, or inverter, is a power electronic device or circuit that transforms direct current (DC) into alternating current (AC). The AC frequency obtained depends on the particular device used. Inverters are the reverse of "converters" which were originally large electromechanical devices that converted alternating current to direct current The input

voltage, the voltage of the inverter, is the same as the output voltage.

The input voltage, output voltage and frequency, and overall power input depend on the design of the specific device or circuit. The inverter does not produce power; the power is supplied by the DC source.

A power inverter can be fully electronic or can be a combination of mechanical effects (such as a rotating device) and electronic circuits. Static inverters do not use moving parts in the conversion process. Power inverters are mainly used in electrical power applications where high currents and voltages are present. Circuits that perform the same function for electronic signals, which usually have very low currents and voltages, are called oscillators.

The inverter is a DC-AC converter, mainly used to supply loads operating with AC voltage when a DC source is available (e.g., batteries) or to inject the energy produced by photovoltaic panels into the grid. There are two types:

- A stand-alone inverter delivers a voltage with a frequency that is either fixed or adjustable by the user. It does not always need the grid to operate; for example, a travel inverter that is plugged into a car's cigarette lighter socket uses the vehicle's 12 V DC to generate 120 or 230 V, 50 or 60 Hz AC.
- A non-autonomous inverter is an all-thyristors rectifier circuit (Graetz bridge) which, in natural switching assisted by the grid, to which it is connected, allows inverter operation (e.g., by recovering energy during braking periods in electric motor vehicles) [14]

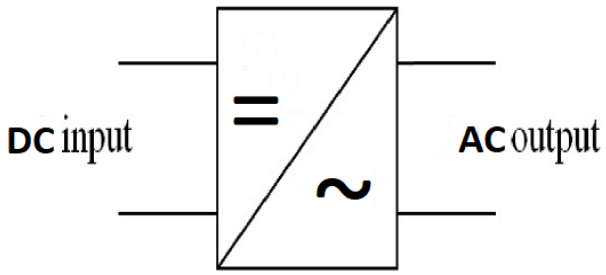

Figure II.3: the inverter synoptic diagram.

II.2.3 Dimmers:

A dimmer is a power electronics device designed to modify an electrical signal in order to vary its effective output voltage and thus modify the power in the load. This device is used on alternating (often sinusoidal) voltages: it is a direct alternating converter.

Dimmers are used to produce dimmers for certain appliances operating on the mains (halogen lamps, domestic Hoovers, hand-held power tools, etc.), for the regulation of electric heating, as well as in many industrial processes (float glass for glass manufacture, heating of fluids in petrochemicals, diffusion furnaces, thermal cycling test benches, etc.). [14].

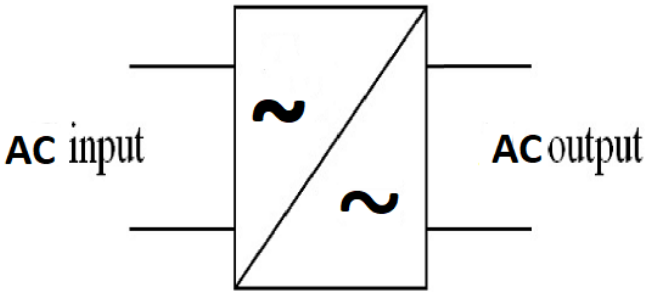

Figure II.4: the dimmer synoptic diagram.

II.2 .1 Cycloconverters:

A cycloconverter is a power electronics circuit that performs direct AC/AC conversion. This means that it can change the frequency of the output signal. It is a form of matrix converter (i.e. for N phases at the input and P phases at the output, NxP bidirectional switches are required). These bidirectional switches are a combination of two thyristors (in anti-parallel), or a triac, whose switching off is done in a natural way with the passage of the current through hem, or one or two IGBTs or RIGBTs. This scheme can also be implemented with bi-directional bi commendable switches (based on a transistor or GTO thyristor), but the term cycloconverter is reserved for those using thyristors. Typically, the input voltage amplitude and frequency are fixed, while the output voltage amplitude and frequency are variable (but this is not mandatory). Unlike indirect converters (rectifier-inverters), a thyristor cycloconverter can only produce a lower frequency than the input. However, the implementation of a matrix converter with advanced "switches" makes it possible to obtain a gain between 0 and infinity (theoretical), identical to a buck-boost circuit. This set-up is rarely used anymore, in particular because of the poor quality of the wave-forms obtained, except for very high powers (a few tens of megawatts and beyond), where its low cost makes its disadvantages disappear.

Figure II.5: the cycloconverter synoptic diagram.

II.2.4 Choppers:

They are DC-DC converters, allowing the variation of a DC voltage to adapt it to the care or to vary the speed of a DC motor or to regulate the brightness of a lamp. The switching is done at a high frequency. It is the analogue, for DC voltage sources, of the dimmer used in AC [13]. If the output voltage is lower than the input voltage, the chopper is said to be a step-down chopper. If the output voltage is lower than the input voltage, the chopper is said to be a step-up chopper (or boost chopper). There are choppers that can work in both ways (Boost-Buck). When the input and output are of different dynamic nature, they can be connected directly (this is called a direct link chopper). When the input and output are of the same dynamic nature, a moment storage element must be used (this is called a storage chopper). Finally, in cases where galvanic isolation of the output from the input is required, so-called "isolated" choppers are used depending on the degree of reversibility required, the structure of the assembly differs [15].

Finally, depending on the power rating of the system, the component technology will differ

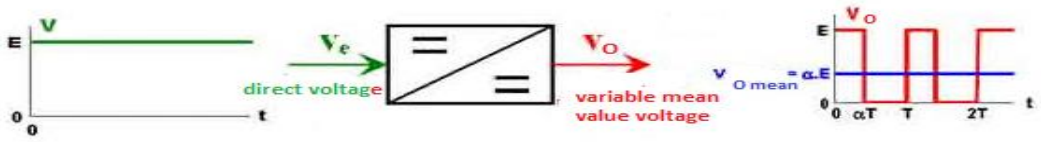

Figure 2.6: the chopper synoptic diagram.

II.2.4.1 Devolving chopper (Buck):

A Buck converter, or series chopper, is a switching power supply that converts This type of converter is used for applications that can be divided into two categories:

- Applications to obtain a fixed (and sometimes regulated) DC voltage from a higher DC voltage Generator.
- Applications to obtain an adjustable voltage, but always lower than the one present at the input [16].

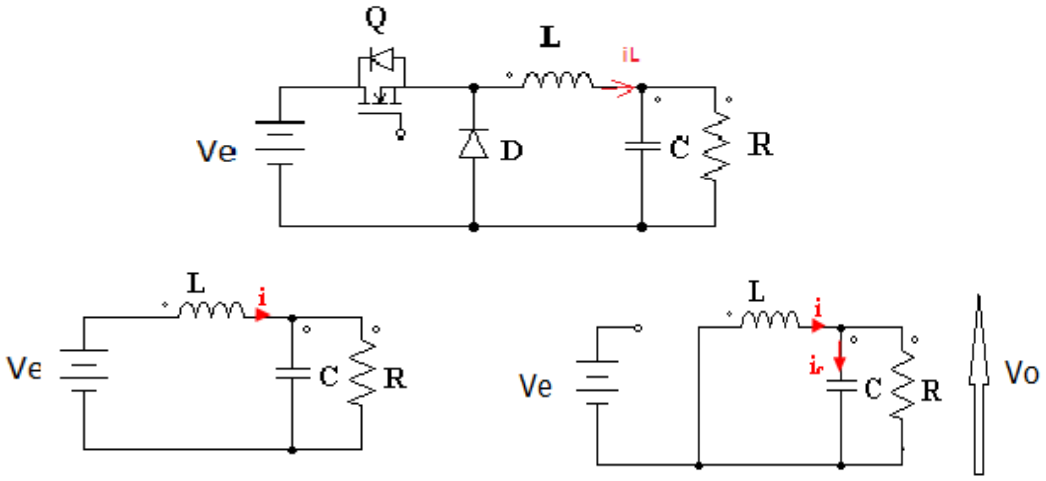

(a) Switch in position u= 1. *(b) Switch in position u= 0.*

Figure II.7: Real devolving converter.

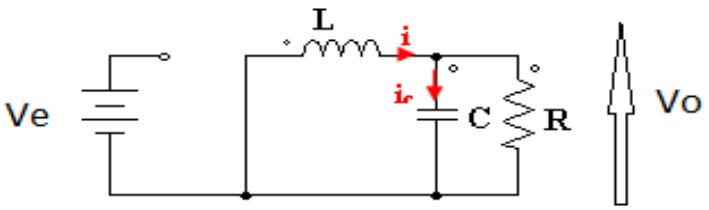

Figure II.8: Circuit topologies of the devolving converter.

a. If we consider that the switch is closed (u=1) and applying Kirchhoff's laws to the circuit we obtain the following equations: [16].

With:

$V_O = Vc$, $i = i_L$

$$L \frac{di}{dt} = V_e - V_o \quad \text{(II.1)}$$

$$C \frac{dV_c}{dt} = i - \frac{V_o}{R} \quad \text{(II.2)}$$

b. For u=0 (the open switch):

$$L \frac{di}{dt} = - V_o \quad \textit{(II.3)}$$

$$C \frac{dV_c}{dt} = i - \frac{V_o}{R} \quad \textit{(II.4)}$$

By comparing the two situations we can obtain a single unified model which is:

$$L\frac{di}{dt} = uV_e - V_o \qquad (II.5)$$

$$C\frac{dV_c}{dt} = i - \frac{V_o}{R} \qquad (II.6)$$

The average buck converter model is described by:

$$L\frac{di}{dt} = uV_e - V_o \qquad (II.7)$$

$$C\frac{dV_c}{dt} = i - \frac{V_o}{R} \qquad (II.8)$$

The characteristics of the currents and the voltage representing the operation of the step-down chopper are given by the following Figures:

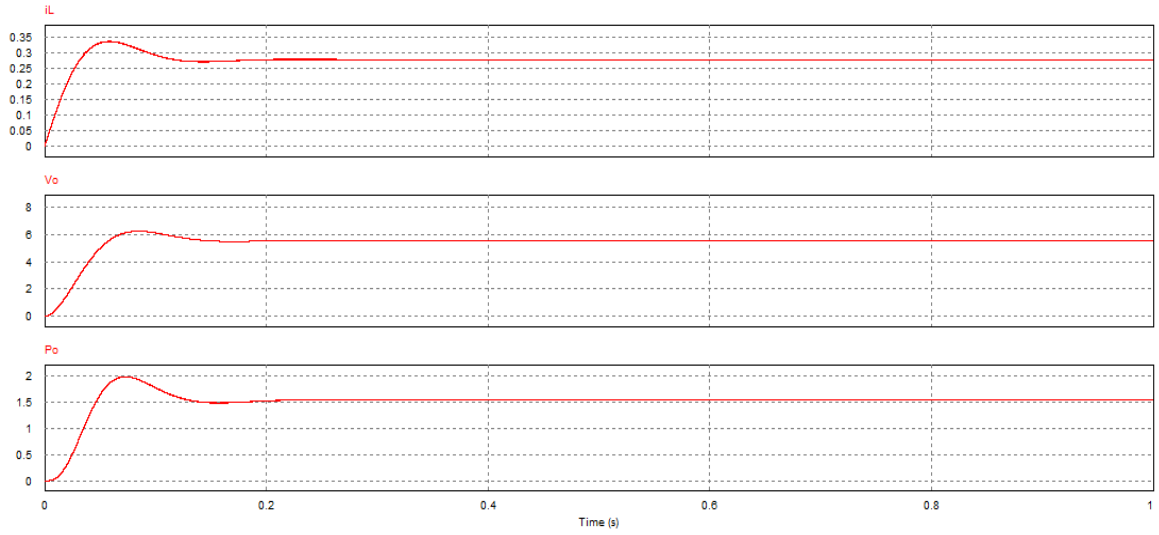

Figure II.9: Characteristic of voltage-current with PSIM.

a) Calculation of the inductance: [17].

When a Buck converter operates in continuous conduction mode, the current IL Through the inductance never cancels. The variation of IL is given by

$$V = L \times \frac{dIL}{dt} \qquad (II.9)$$

where Q1 is on, is defined by the duty cycle (D) and the switching frequency (F_{SW})

$$\boldsymbol{D = F_{sw} \times \Delta t = \frac{V_o}{V_e}} \quad \text{(II.10)}$$

The expression for L can therefore be rewritten as follows:

$$\boldsymbol{L = (V_e - V_o) \times \frac{D/F_{SW}}{\Delta I_L}} \quad \text{(II.11)}$$

Ve = typical input voltage

Vo = desired output voltage

F_{SW} = minimum switching frequency of the converter

ΔI_L = estimated inductor ripple current, see the following:

A Good estimation for the inductor ripple current is 20% to 40% of the output current.

$\Delta L_L = (0.2 \text{ to } 0.4) \times I_{OUT(max)}$

Δ_{IL} = estimated inductor ripple current

$I_{Out(max)}$ = maximum output current necessary in the application

b) Calculation of the capacitor [17]:

The input capacitor defines the residual input ripple. The result is

$$\boldsymbol{C_{OUT\,(min),OS} = \frac{\Delta I_{OUT}^2 \times L}{2 \times V_{OUT} \times V_{Os}}} \quad \text{(II.12)}$$

C_{OUT} (min), OS = minimum output capacitance for a desired overshoot

ΔIOUT = maximum output current change in the application

VOUT = desired output voltage

VOS = desired output voltage change due to the overshoot

c) Calculation of the average value of V_O [17]:

$$\boldsymbol{V_{omoy} = \frac{1}{T}\int_0^{\cdot} V_e(t)\,dt = \alpha V_e} \quad \text{(II .13)}$$

II.2.4.2 Boost chopper:

A boost converter (or step-up converter) is a switching power supply that converts a DC voltage into another DC voltage of higher value. A boost converter is used when it is desired to increase the available voltage of a DC source [26]. Its basic schematic is shown in figure (2.10).

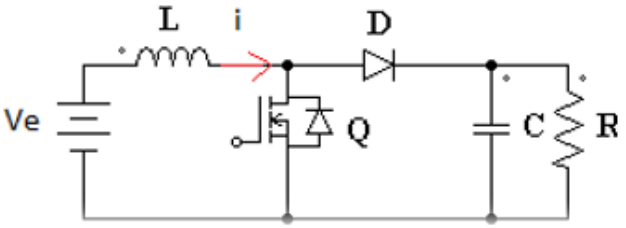

Figure II.10: Actual boost converter.

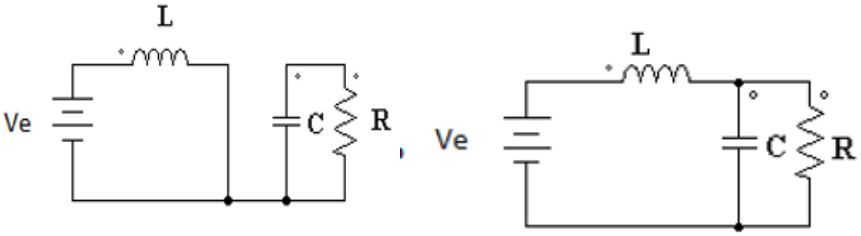

(a) Switch position u= 1 ***(b) Switch position u= 0***

Figure II.10: Circuits of the boost converter topologies.

a) If we consider that the switch is closed (u=1) and applying Kirchhoff's laws to the circuit we obtain the following equations:

$$L\ \frac{di}{dt} = Ve \qquad (II.14)$$

$$C\frac{dVc}{dt} = \frac{Vo}{R} \qquad (II.15)$$

b) When the switch is open (u=0) we obtain the following dynamics:

$$L\ \frac{di}{dt} = Ve - Vo \qquad (II.16)$$

$$C\frac{dVc}{dt} = i - \frac{Vo}{R} \qquad (II.17)$$

By comparing the two situations we can obtain a single unified model which is:

$$\boldsymbol{L}\, di/dt = Ve - (1-u)Vo \qquad (II.18)$$

$$C\, dVc/dt = (1-u)i - Vo/R \qquad (II.19)$$

The characteristics of the charging current and voltage are given in the Figure below:

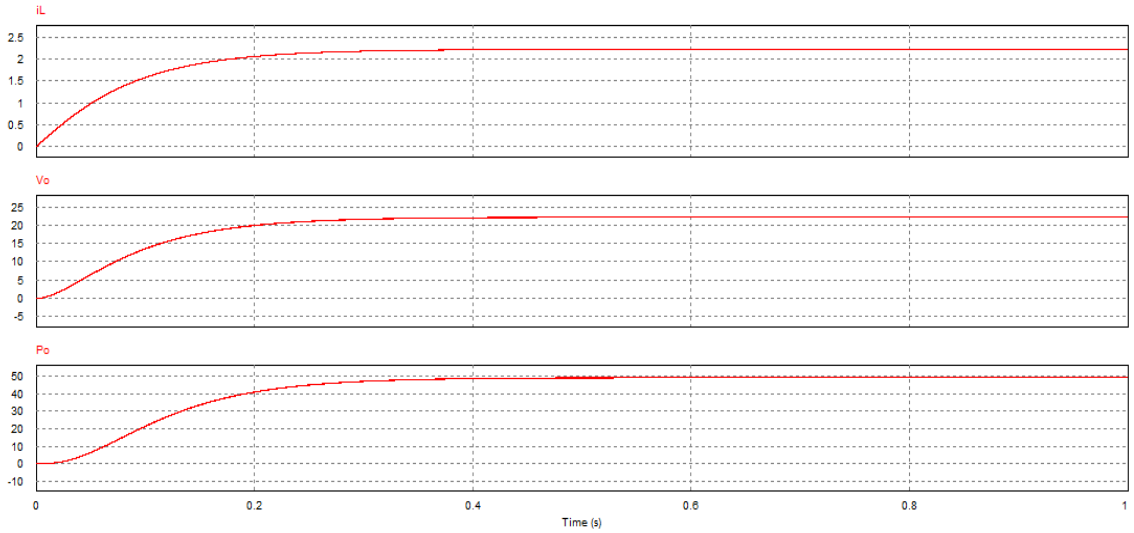

Figure II.11: Characteristic of the voltage and current of the BOOST converter with PSIM.

a) Calculation of the inductance [17]:

The value of L is calculated by the following relationship:

$$L = \frac{V_e \alpha}{f DI} \qquad (II.20)$$

b) Calculation of the capacitor [17]:

During phase 1, which lasts for α T, the capacitor alone supplies energy to the load. The current is assumed to be constant; the charge supplied by the capacitor can be calculated capacitor:

$$\boldsymbol{\Delta Q = I_o \alpha T} \qquad (II.21)$$

If we assume a ripple ΔVo of the output voltage, we can write:

$$\boldsymbol{\Delta Q = C D V_o} \qquad (II.22)$$

The capacitance of the output capacitor can be deduced from this:

$$C = \frac{I_o \alpha T}{DVo} \quad \text{(II.23)}$$

$$L = (V_e - V_o) \times \frac{D/F_{SW}}{\Delta I_L} \quad \text{(II.24)}$$

Ve = typical input voltage

VO = desired output voltage

F_{SW} = minimum switching frequency of the converter

Δ_{IL} = estimated inductor ripple current

I_O=output current necessary in the application

c) Calculation of the average value of Vs [17]:

$$Vo_{moy} = \frac{1}{T}\int_0^{\alpha t} Ve(t)\,dt = (1-\alpha)Ve \quad \text{(II.25)}$$

II.2.4.3 Buck-Boost Chopper:

A Buck-Boost converter is a switching power supply that converts one DC voltage into another DC voltage of lower or higher value but of opposite polarity. A disadvantage of this converter is that its switch does not A disadvantage of this converter is that its switch does not have a terminal connected to ground, thus complicating its control [16]. Figure (2.13) shows the schematic diagram of the Buck-Boost converter.

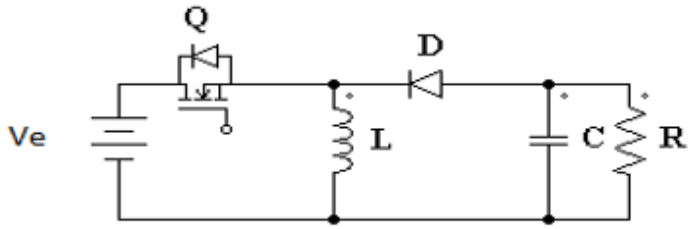

Figure II.12: Real devolver-to-volver converter.

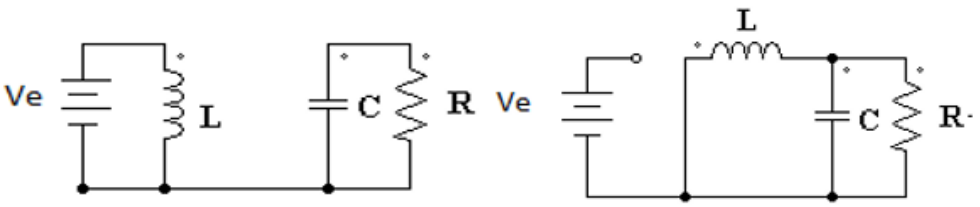

(a) Switch position u= 1 *(b) Switch position u= 0*

Figure II.13: Circuits of the Buck-Boost converter topologies.

a) If we consider that the switch is closed (u=1) and applying Kirchhoff's laws to the circuit we obtain the following equations:

$$L\ (di)/(dt) = Ve \qquad (II.26)$$

$$C\ dVc/dt = -Vo/R \qquad (II.27)$$

.

b) When the switch is open (u=0) we obtain the following dynamics:

$$L\ \frac{di}{dt} = Vo \qquad (2.28)$$

$$C\frac{dVc}{dt} = -i - \frac{Vo}{R} \qquad (2.29)$$

..

Comparing the two dynamics we obtain the following switched model:

$$L\ \frac{di}{dt} = (1-u)Vo + uVe \qquad (2.30)$$

$$C\ \frac{dVc}{dt} = -(1-u)i + \frac{Vo}{R} \qquad (2.31)$$

The characteristics of the charging current and voltage are given in the Figure below:

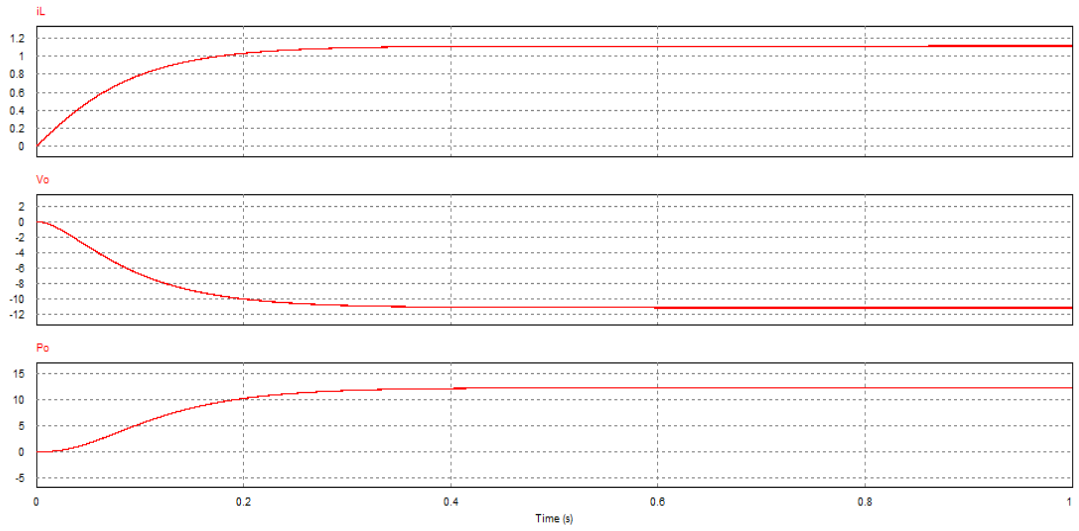

Figure II.14: Characteristic of the voltage and current of the Buck-BOOST converter.

a) Calculation of the inductance [17]:

The next step is to select the required inductance. If the inductance range is not limited by the IC you can estimate the required inductance based on the well-known differential equation:

$$L = \frac{V_e \Delta}{I_L F_{sw}} \quad \text{(II.32)}$$

$$I_L = \frac{I_0}{1-\Delta} \quad \textit{(II.33)}$$

b) Calculation of the capacitor :

$$\boldsymbol{C = \frac{I_L \Delta}{f_{SW}(V_e - I_L)}} \quad \text{(II.34)}$$

Ve = typical input voltage

F_{SW} = minimum switching frequency of the converter

I_O=output current necessary in the application

c) Calculation of the average value of Vs:

$$\boldsymbol{Vo_{moy} = \frac{1}{T}\int_0^{\cdot} Ve(t)\, dt}$$

$$= V_e \frac{\alpha}{1-\alpha} \quad \text{(II.35)}$$

II.3 Conclusion:

In this chapter, we have presented the most commonly used DC/DC converters in the form of matching stages (Buck, Boost and Buck-Boost). With a simulation of input and output voltages by the PSIM software, we will study in the following chapter our control with buck converter.

CHAPTER III :

MPPT Controls & the PV System Simulation

III.1 Introduction:

Specific control laws exist to cause devices to operate at maximum points of their characteristics without these points being known a priori, or without knowing when they were changed or the reasons for the change.

In the case of energy sources, this translates into maximum power points.

This type of control is often referred to in the literature as Maximum Power Point Tracking (MPPT).

In this chapter, we will see the principle and the classical study of the most known three controls that we chose from many several controls for the maximum power point (MPP) while ensuring a perfect match between the generator and its load in order to transfer the maximum power then we implemented those techniques in the psim software to see their performance after applying some perturbations in the temperature and the irradiation. [18]

III.2 Maximum Power Point Tracking (MPPT):

III.2.1 Principle:

In order for the photovoltaic system to operate at maximum power points of their characteristics, there are specific control laws that meet this need.

This control is referred to in the literature as Maximum Power Point Tracking (MPPT). The principle of these controls is to search for the maximum power point (MPP) while keeping a good adaptation between the generator and its load to ensure the transfer of the maximum power.

Figure (III.1) shows an elementary photovoltaic conversion chain associated with an MPPT control.

The MPPT control is associated with a static converter that allows the adaptation between the GPV and the load so that the generated power corresponds to its maximum value and is transferred directly to the load [18].

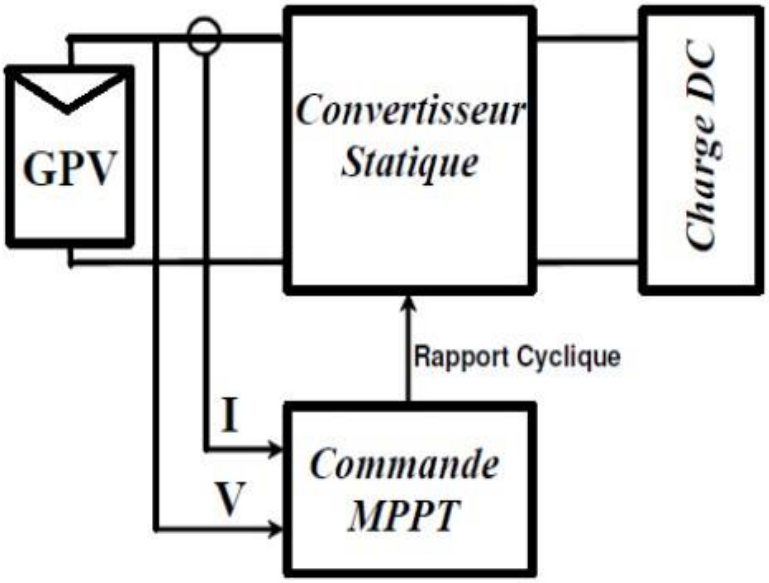

Figure III.1: Photovoltaic conversion chain with static converter controlled by MPPT control.

III.2.2 MPPT control techniques:

There are many MPPT control methods and techniques available in the literature:

Perturb and Observe (P&O), conductance incrementing (IncCond) and Hill Climbing method [28].

Currently there are methods based on artificial intelligence, namely fuzzy logic, neural networks and genetic algorithms.

III.2.2.1 The Perturb & Observe (P&O) method:

a) The P&O principle:

The principle of P&O MPPT controls consists of perturbing the VPV voltage by a small amount around its initial value and analyzing the behavior of the resulting PPV power variation. Thus, as shown in figure (III.2), it can be deduced that if a positive increment of the VPV voltage results in an increase of the PPV power, this means that the operating point is to the left of the MPP.

If, on the other hand, the power decreases, it implies that the system has passed the MPP. A similar reasoning can be made when the voltage decreases. From these various analyses of the consequences of a voltage variation on the PPV (VPV) characteristic, it is then easy to locate the operating point in relation to the PPM and Converge the latter towards the maximum power through a control command [19].

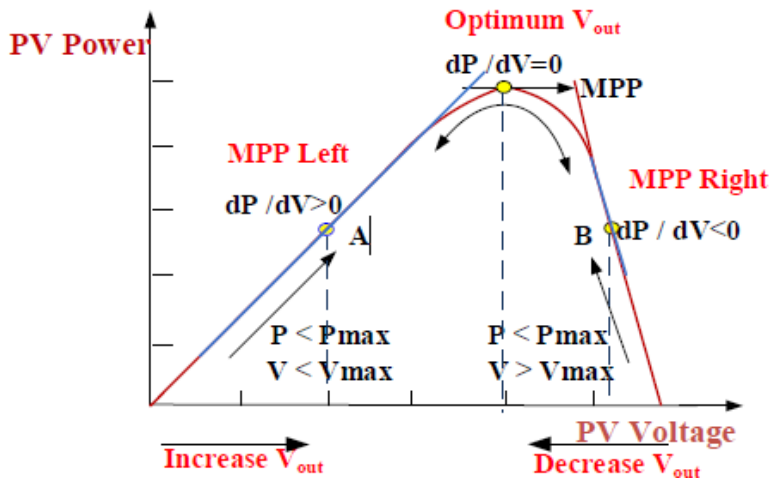

Figure III.2: P&O three modes of operation.

Figure (III.3) shows the classical algorithm associated with a P&O MPPT control, where the power evolution is analyzed after each voltage disturbance. For this type of control, two sensors (GPV current and voltage) are needed to determine the PV power at each instant.

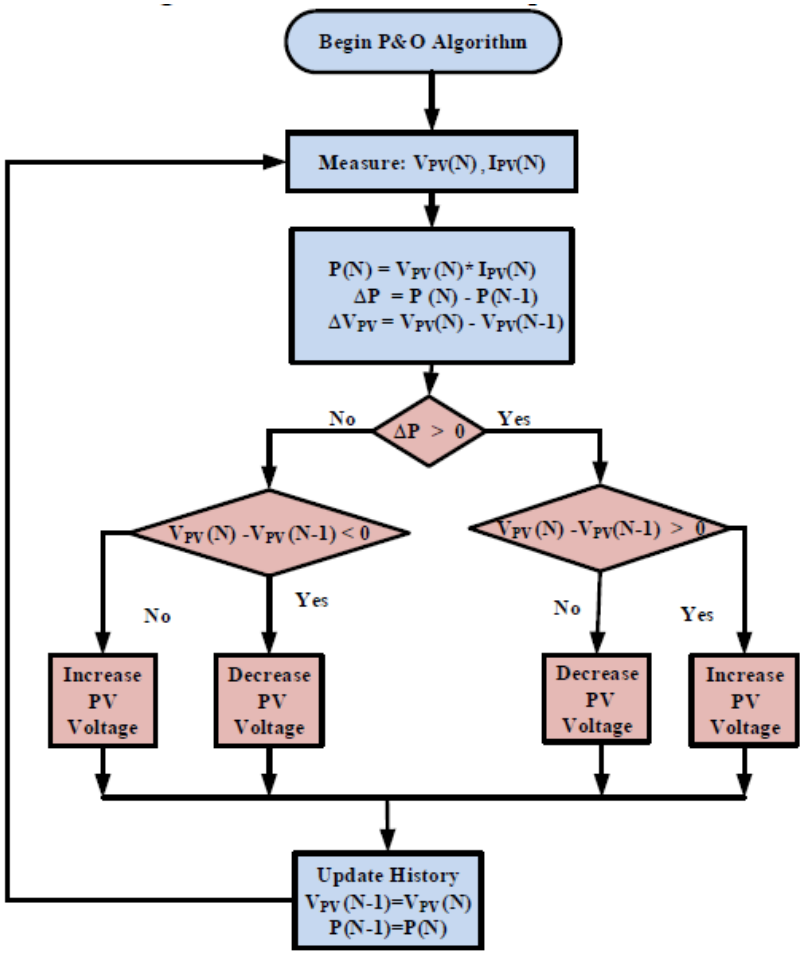

Figure III.3: The P&O algorithm flowchart.

Such as:

Ppvn: the new power

Ppvn-1: the anceinne power in time (t-1).

$$\Delta V = V_{PVn} - V_{PVn-1} \quad (III.1)$$

$$\Delta P = P_{pvn} - P_{PVn-1} \quad (III.2)$$

Because of its ease of implementation, the P&O method is frequently used despite the fact that it presents problems of oscillation around the PPM because the search must be repeated periodically to force the system to oscillate around the PPM. In addition, and for abrupt changes in climatic conditions or/and load, this method is sometimes misinterpreted as to the direction in which the MPP should be achieved. [19]

b) Simulation of P&O using Psim:

As a first step, the basic P&O algorithm is implemented using analog blocks figure (III.4), it is simulated in PSIM software as shown in figure (III.5) and the results shown in figure (III.6) This method (P&O) generates oscillation in the output power; therefore, its efficiency is not at the requested level (96.6%).

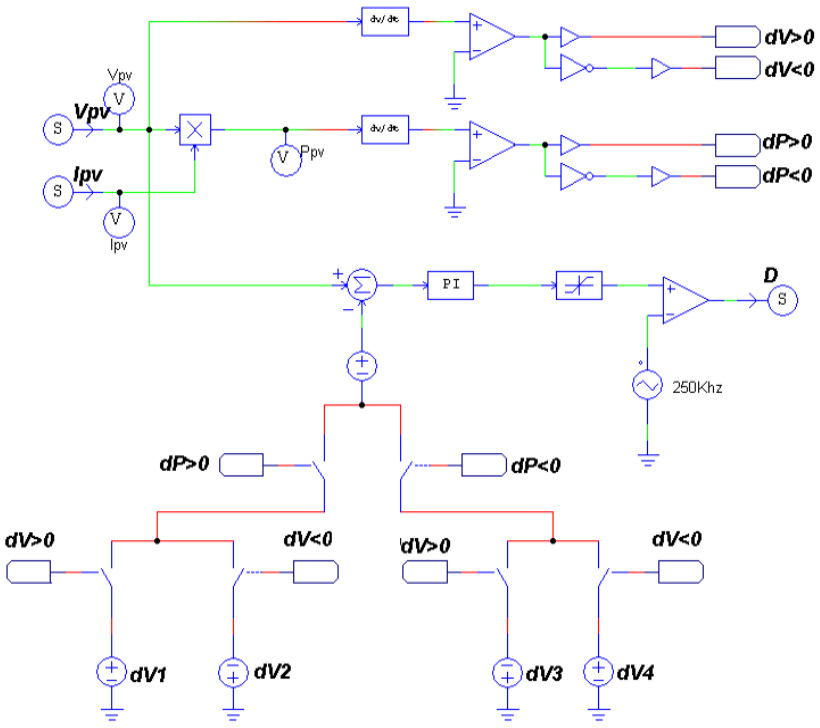

Figure III.4: model of the P&O technique in psim.

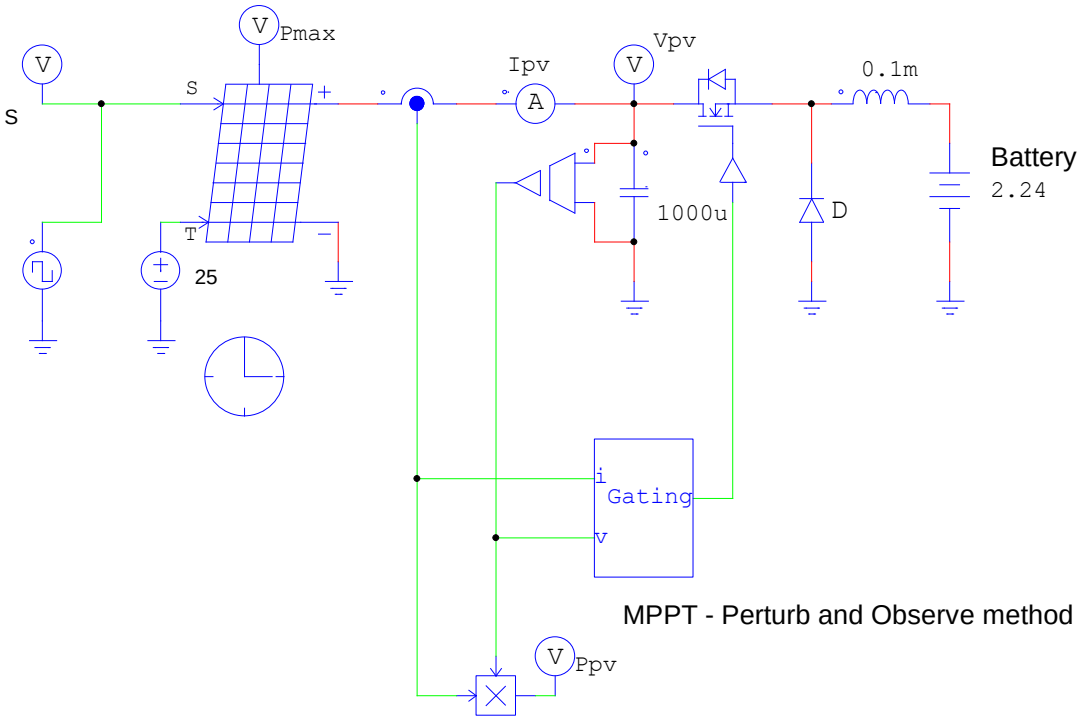

Figure III.5: model of the PV system using the P&O method.

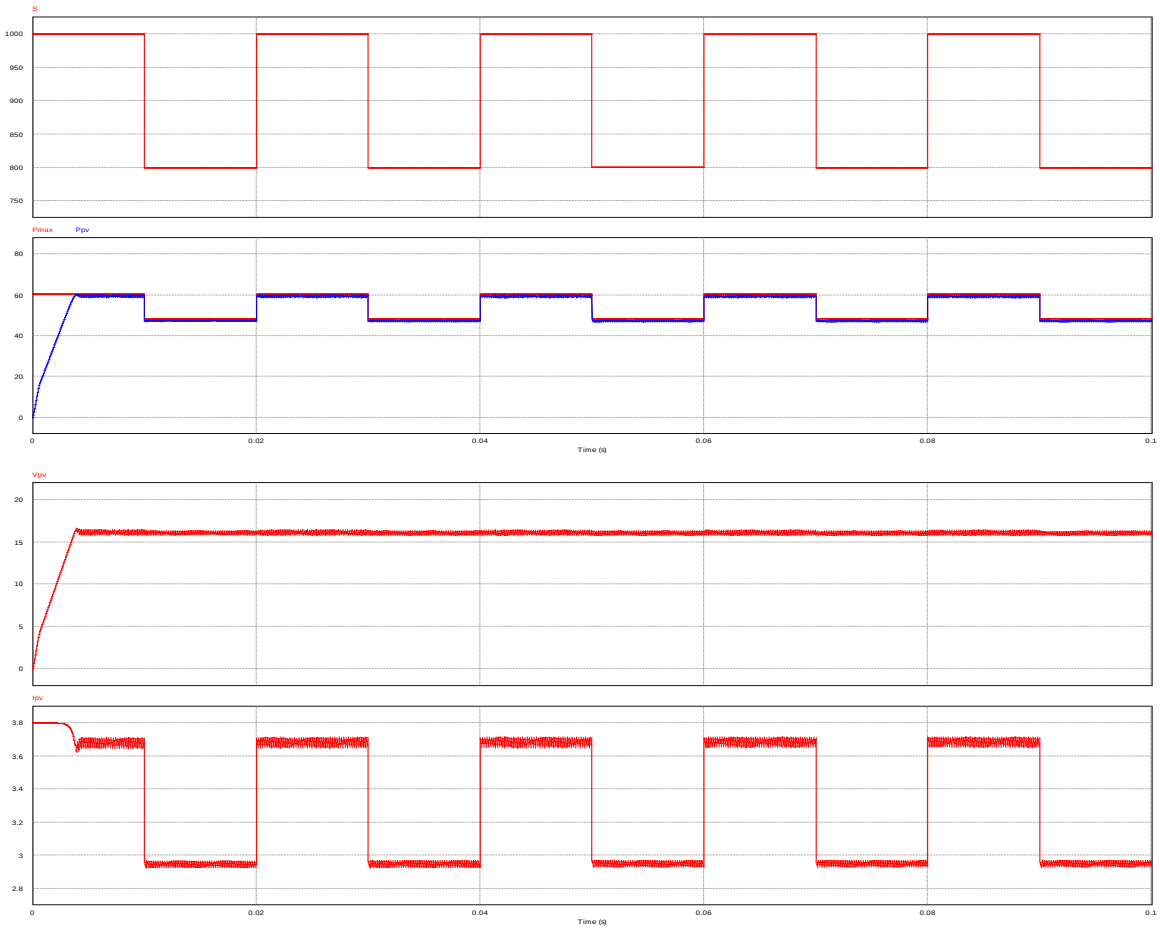

Figure III.6: results of the PV system simulation.

So the figure (III.6),shows the results of the P&O algorithm simulation after implementing it

in the PSIM software.The graph represents the radiation,the comparison between the maximum and the load powers, the current and the voltage respectively on the Y axis, while the time appear on the X axis.it maybe seen clearly that the voltage rose steadily at first and then stabilize at its maximum range so that it compensate the current whenever it dropped off. For the powers ,the load power is tracking down the maximum power while its changing according to the perturbation (irradiation) we have applied trying to reach the maximum power point.

III.2.2.2 The Incremental Conductance Method (IncCond):

a) INC principle:

This technique is based on the variation of the conductance of the GPV and its influence on the operating point position. The conductance and the elementary variation of the conductance (increment) of the photovoltaic module are defined respectively by:

$$G = \frac{I_{pv}}{V_{pv}} \quad (III.3)$$

$$dG = \frac{dI_{pv}}{dV_{pv}} \quad (III.4)$$

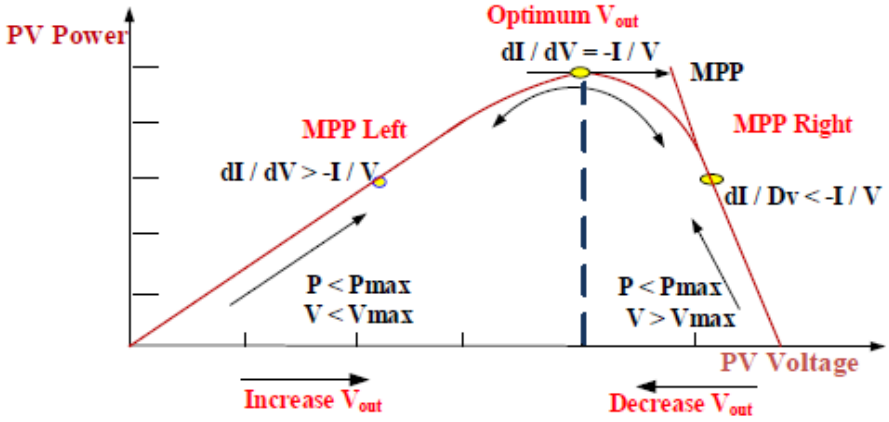

Figure III.7: INC algorithm power - voltage curve.

The IC method is built on the power-voltage slope as exposed in figure (III.4). The power-voltage characteristic of the GPV allows us to write the following conditions:

If $dPpv/\ dVpv > 0$ the operating point is to the left of the MPP.

If $dPpv/\ dVpv = 0$ the operating point is on the MPP.

If $dPpv/\ dVpv < 0$ the operating point is to the right of the MPP.

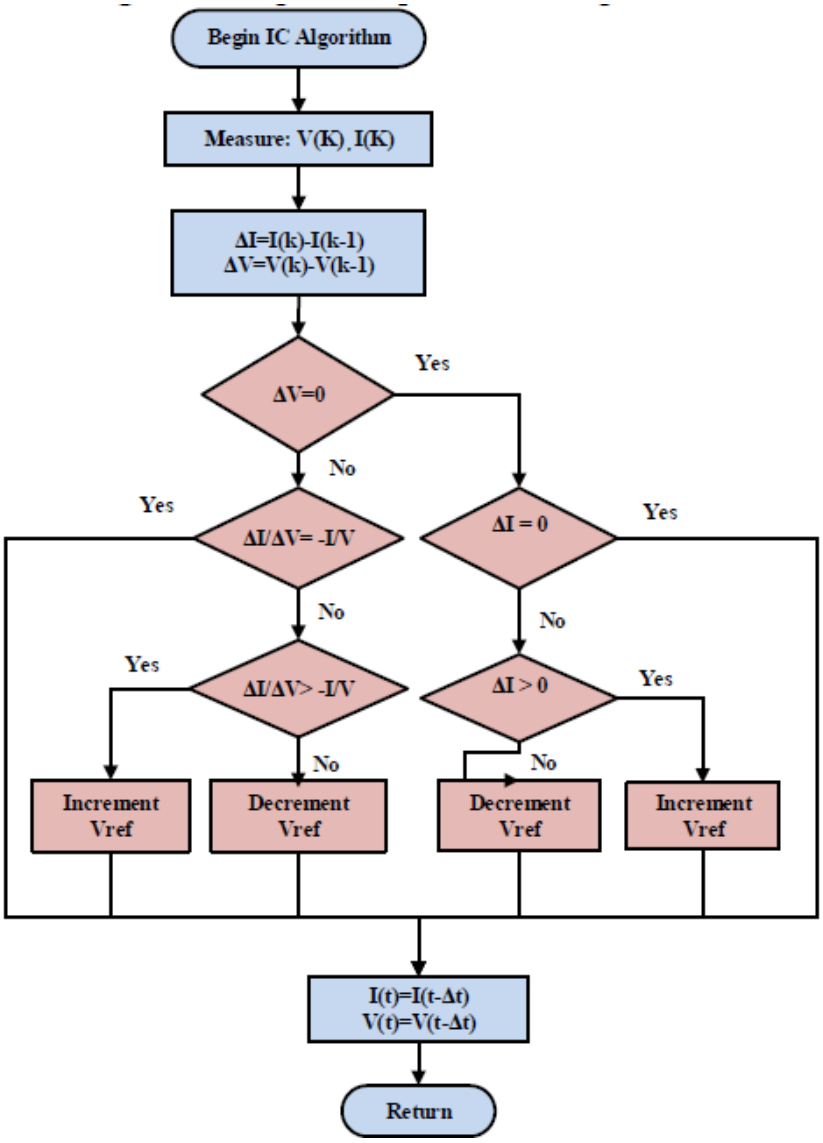

Figure III.8: the INC algorithm flowchart.

Practically, like the P&O method, this technique exhibits oscillations around the MPP because it is difficult to meet the Condition $\frac{dP_{pv}}{dV_{pv}}=0$, so the system is always looking for it. The

IncCond algorithm is more complex than the P&O algorithm, which results in a longer execution time. [20]

b) Simulation of the INC technique using psim:

The INC algorithm is implemented using analog blocks figure (III.9), it is simulated in PSIM software as shown in figure (III.10) and the results shown in figure (III.11).

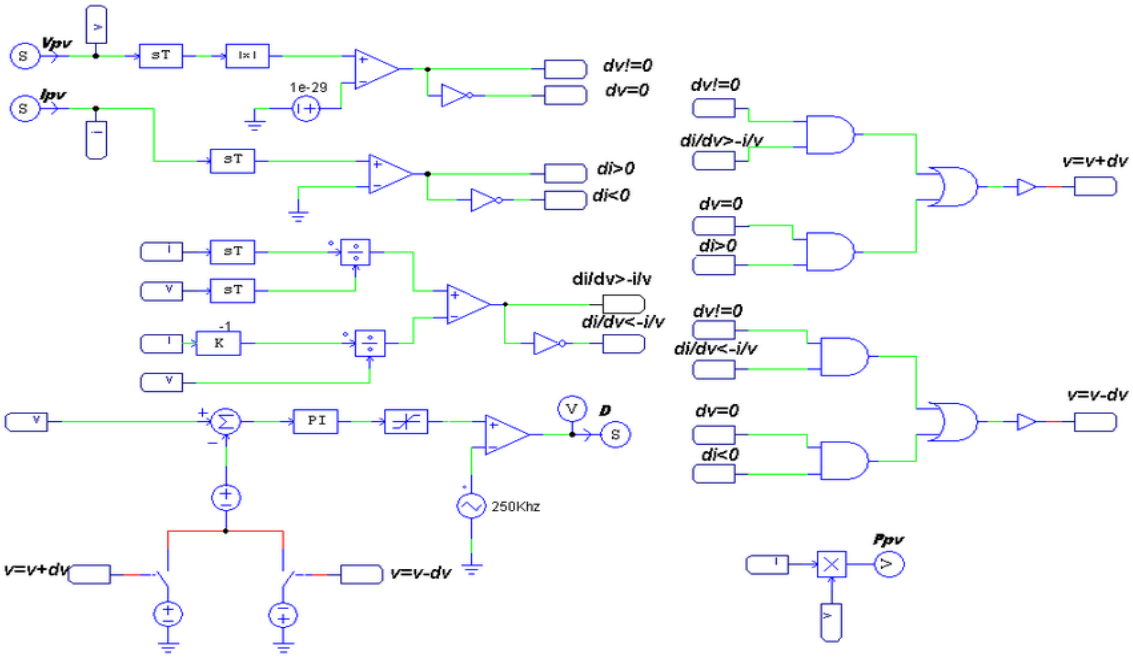

Figure III.9: model of the INC technique in Psim.

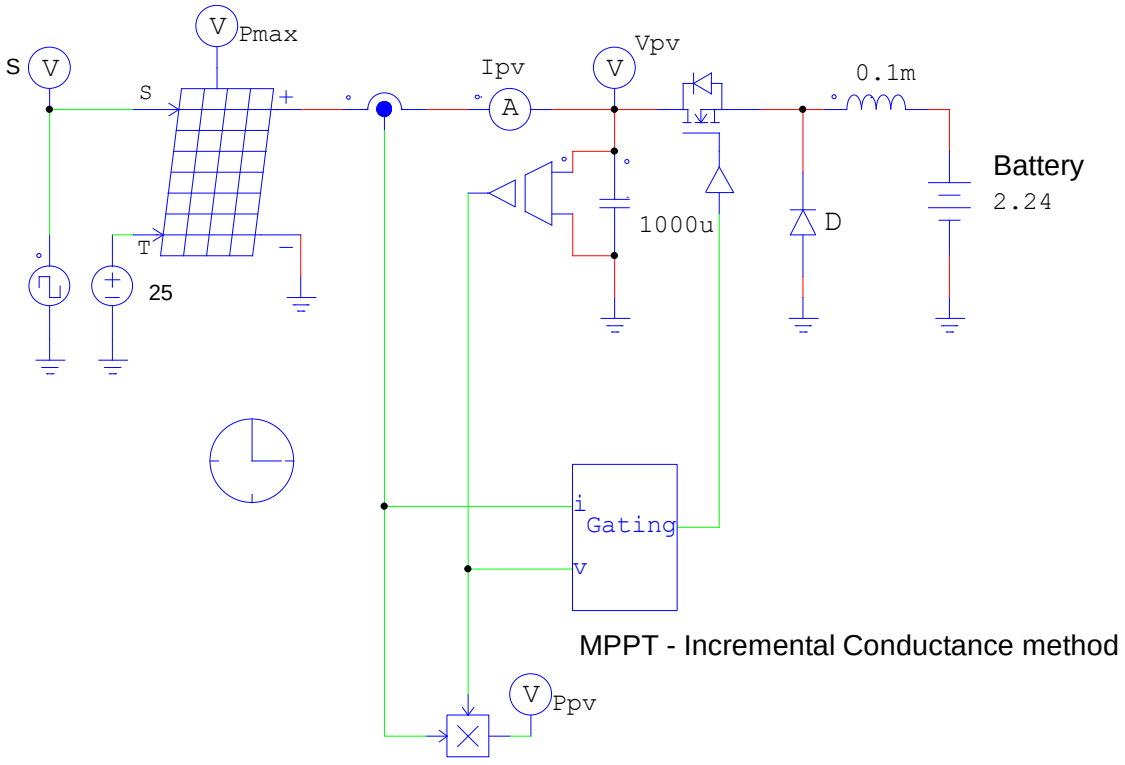

Figure III.10: model of the PV system using the INC method.

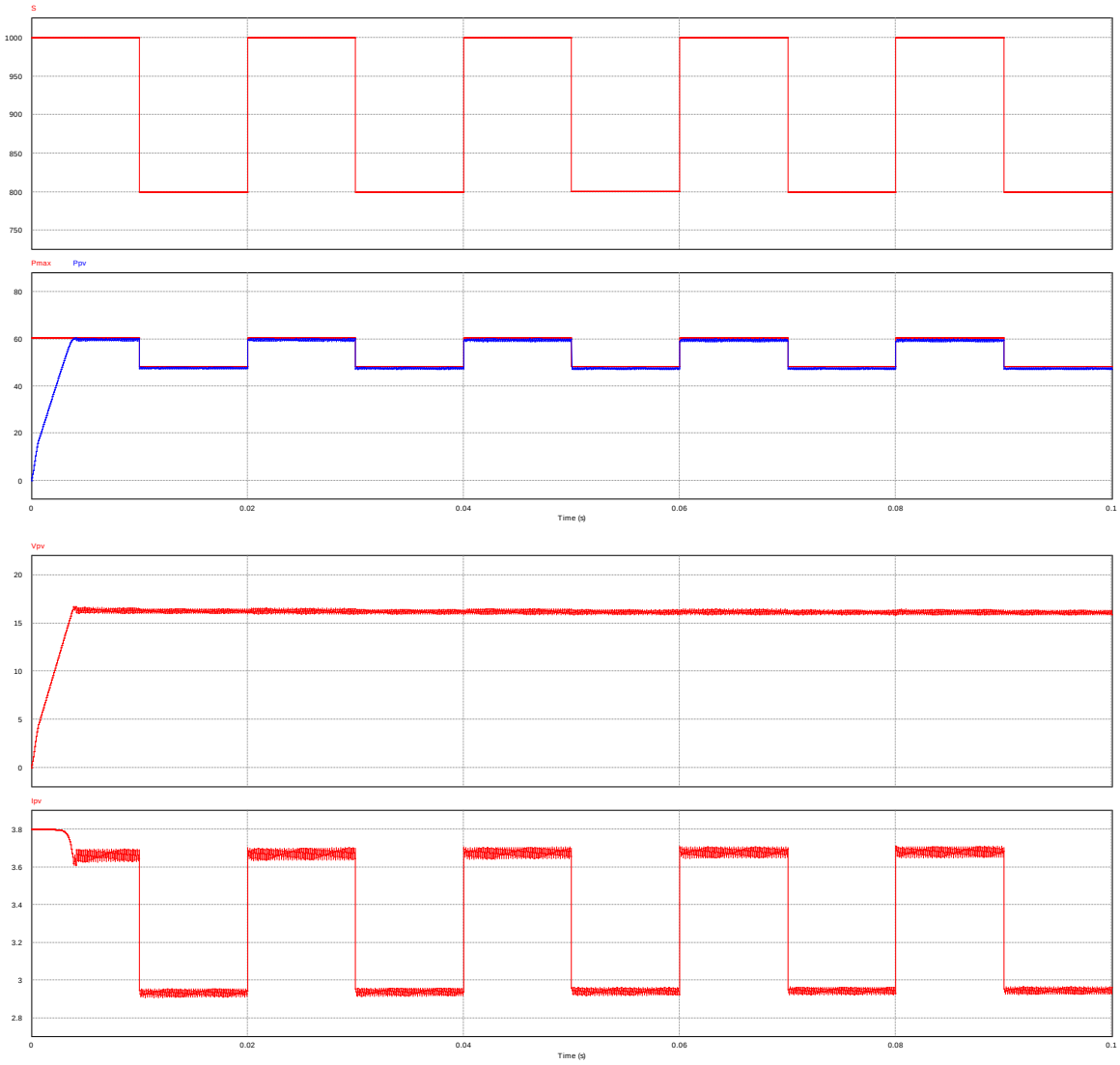

Figure III.11: results of the PV system simulation.

The performance of the INC algorithm is examined through the irradiation changes covering different cases. Figure (III.11), presents the test result of the INC algorithm. Therefore, as shown there is a slightly difference according to the first technique.in addition, the INC detects the fast increase of irradiation and performs a correct decision in duty cycle.

III.2.2.3 Hill climbing method:

a) Hill climbing principle:

The control technique called Hill Climbing [20] consists of "climbing" the operating point along the generator characteristic with a maximum. For this purpose, two slopes are possible. The search theoretically stops when the maximum power point is reached. This method is based on the power versus duty cycle characteristic P(D). Mathematically, the

mpp is reached $\Delta Ppv / \Delta D = 0$ when as shown in figure (III.11).

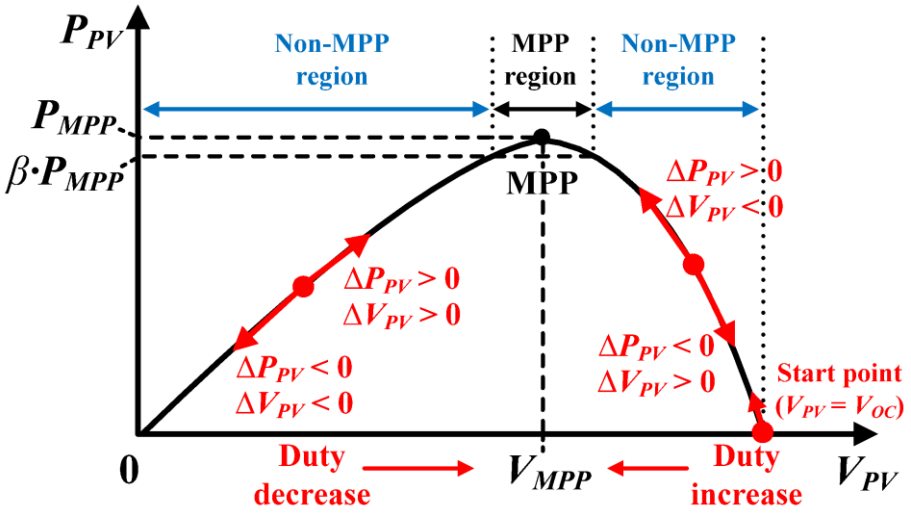

Figure III.11: Relationship between PPV and duty cycle D of the static .

The algorithm for this method is shown in Figure (III.12) Hill Climbing involves a disturbance in the duty cycle of the power converter. In the case of a GPV connected to a power converter, the disturbance in the duty cycle of the power converter disturbs the PV array current and consequently disturbs the PV array voltage [20]. The increment

(decrement) of the voltage increases (decreases) the power when used on the left side of the MPP and decreases (increases) the power when used on the right side of the MPP. Therefore, if there is an increase in power, the subsequent perturbation should be kept the same to reach the MPP and if there is a decrease in power, the perturbation should be reversed. The process is repeated periodically until the MPP is reached. The system then oscillates around the MPP. The oscillation can be reduced by reducing the disturbance step size. However, a smaller disturbance size slows down the MPPT [19].

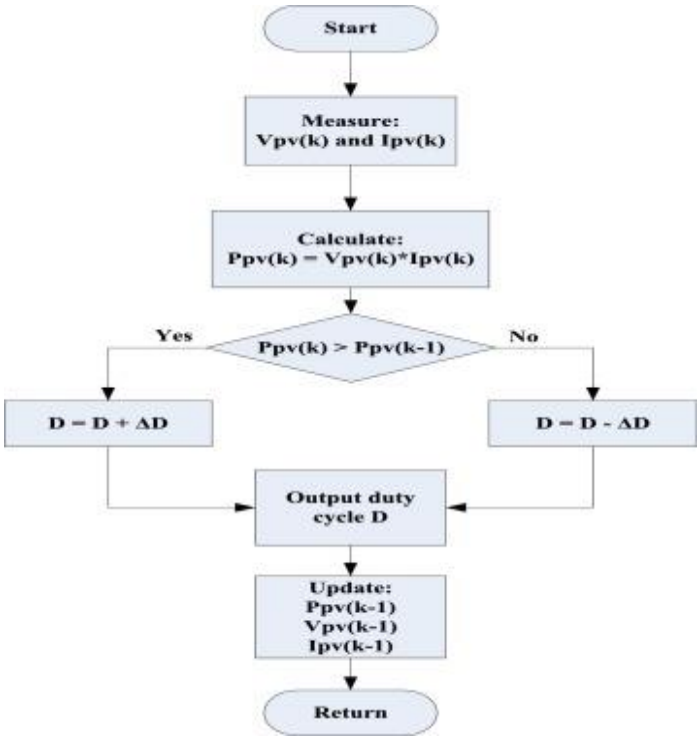

Figure III.12: the hill climbing algorithm flowchart.

The advantage of the latter technique is that it is simple to implement. On the other hand, it has the same disadvantages as the P&O method concerning oscillations around the PPM in the steady state and an occasional loss of the MPP search when the climatic conditions change rapidly [20].

b) Simulation of the hill climbing technique using Psim[21]:

The INC algorithm is implemented using analog blocks figure (III.9), it is simulated in PSIM software as shown in figure (III.10) and the results shown in figure (III.11).

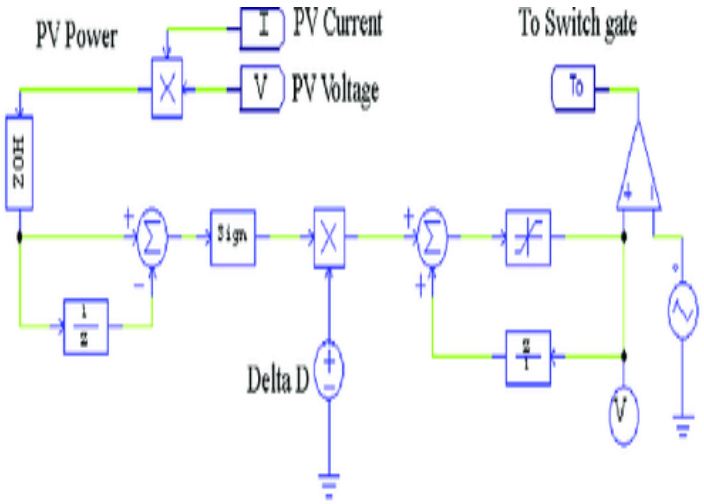

Figure III.13: Model of the INC technique in Psim.

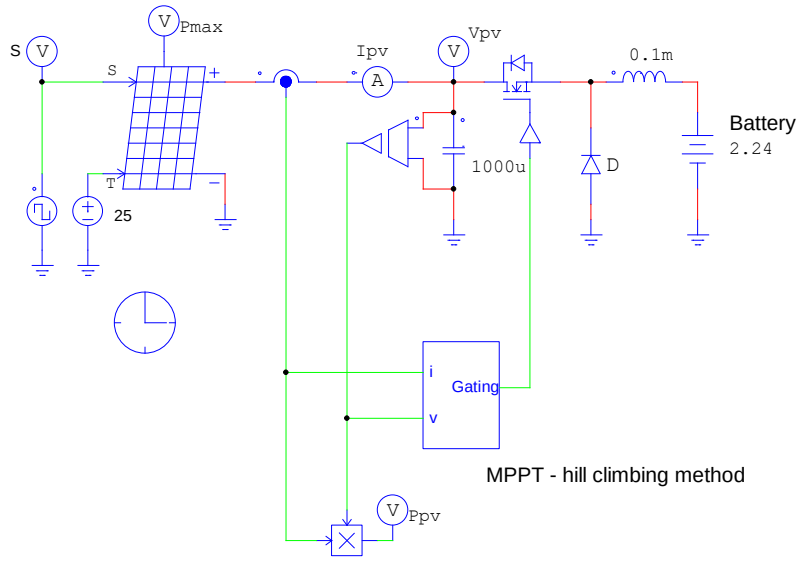

Figure III.14: Model of the PV system using the INC method.

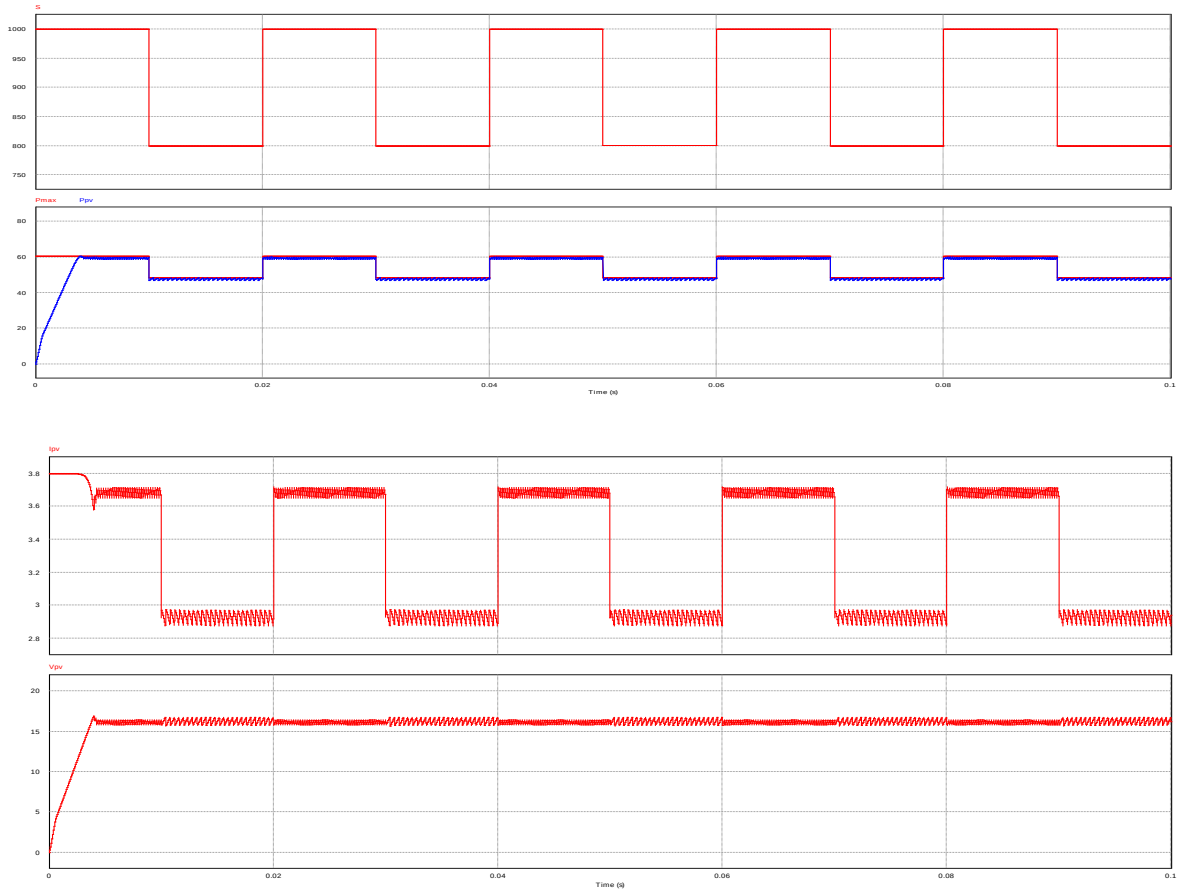

Figure III.15: results of the PV system simulation.

As shown in Figure (III.15) the pv panel power is following the maximum power like we have seen in the previous cases while the irradiation disturbance is applied in order to reach the highest level of power occurred by the solar panel and performs the correct decision in duty cycle. [22,23].

III.2.3 Comparative study:

The following table represents a comparative study between the classical MPPT control techniques "Perturb & Observe", "Incremental conductance" and" hill climbing".

Table III.1: Comparison of the MPPT P&O and IncCond techniques [31].

Algorithms MPPT.	P&O	IncCond	Hill climbing
Type of sensors used.	1 voltage. 1 current.	1 voltage. 1current.	1 voltage. 1current.
Identification of PV panel parameters	Not necessary.	Not necessary.	Not necessary
Complexity.	Lower	Medium.	medium
Convergence speed.	Medium.	Medium.	medium
Precision.	96.6%	97.07%	95%

III.2.4 Remarks and interpretations:

After this study, according to the advantage of the P&O method and its simplicity and the ease of implementing its algorithm according to the other techniques. It will be used and simulated in our system.

III.3 Conclusion:

In this chapter, we have seen the classical study of the most famous techniques (P&O, INC, HC), which are necessary for a photovoltaic system to operate at its maximum power even for weather or load variations. Then we have implemented those techniques in the psim software in order to see their performance in the real time.

CHAPTER IV :

Simulation & Realization of the MPPT Regulator& the PV System

IV.1 Introduction:

This chapter, for the simulation and the practical study of a photovoltaic system adapted with a digital MPPT "perturbation and observation" control.

The realization of the system is based on the dimensioning and the technical characteristics of the elements available in the electronics laboratory of the university Abbes Laghrour of Khenchela.

The experimental setup of a complete PV system (GPV+Buck+MPPT+load) is described.

All the simulation operations are done by the Proteus 8 software.

IV.2 Simulation of the different components of the system in Proteus

IV.2.1 Simulation of the buck converter:

Figure (IV.1) shows the schematic of the buck converter under Proteus. The following tests are carried out tests on the operation of the buck converter and its voltage decline. The converter is working well, the decrease of the duty cycle decreases the output voltage and vice versa.

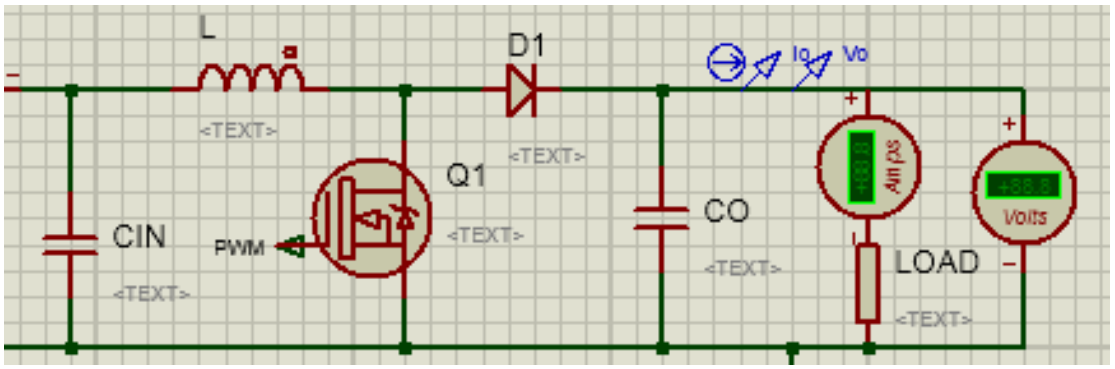

Figure IV.1: Diagram of the buck converter under Porteous.

IV.2.2 Simulation of the voltage sensor:

Figure (IV.2) shows the simulation of the voltage sensor under Proteus. This

This simulation is performed under Proteus; it shows the efficiency of this sensor to measure a DC voltage from a DC voltage.

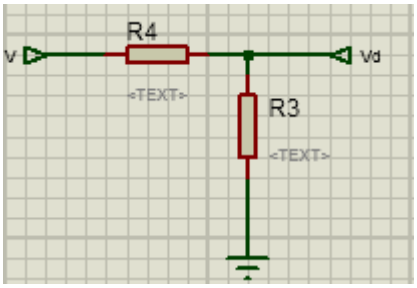

Figure IV.2: Diagram of the voltage sensor in Proteus.

IV.2.3 Simulation of the current sensor:

Figure (IV.3) shows the schematic of the current sensor in Proteus. A simulation has been a simulation was carried out in Proteus to measure a DC current. This simulation shows the sensitivity of this sensor for measuring current.

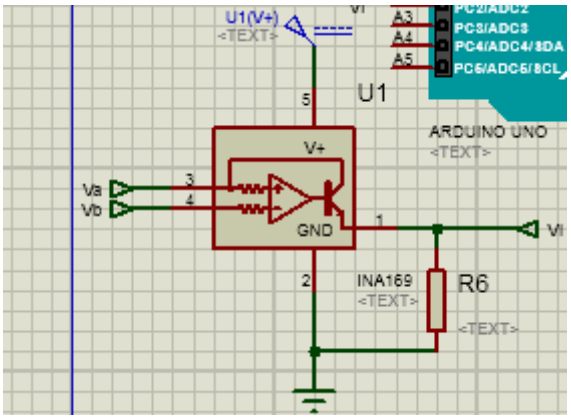

Figure IV.3: Diagram of the current sensor in Proteus.

IV.2.4 Simulation of an LCD display:

The diagram of an LCD display under Proteus is shown in figure (IV.4). This display represents the results obtained.

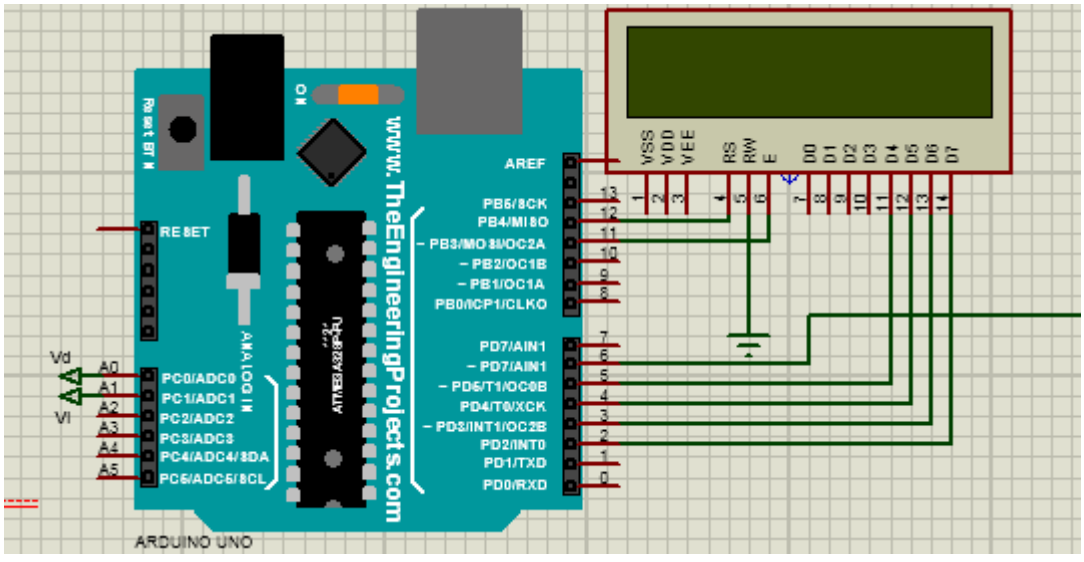

Figure IV.4: Schematic of LCD display in Proteus.

IV.2.5 Simulation of the PV panel:

In order to model a PV panel in Proteus tool, its equivalent circuit is done with a controlled

current source and a diode with modified Spice code, that in order to design a real model of PV panel. Figure (IV.5) presents the Proteus model and its Spice code.

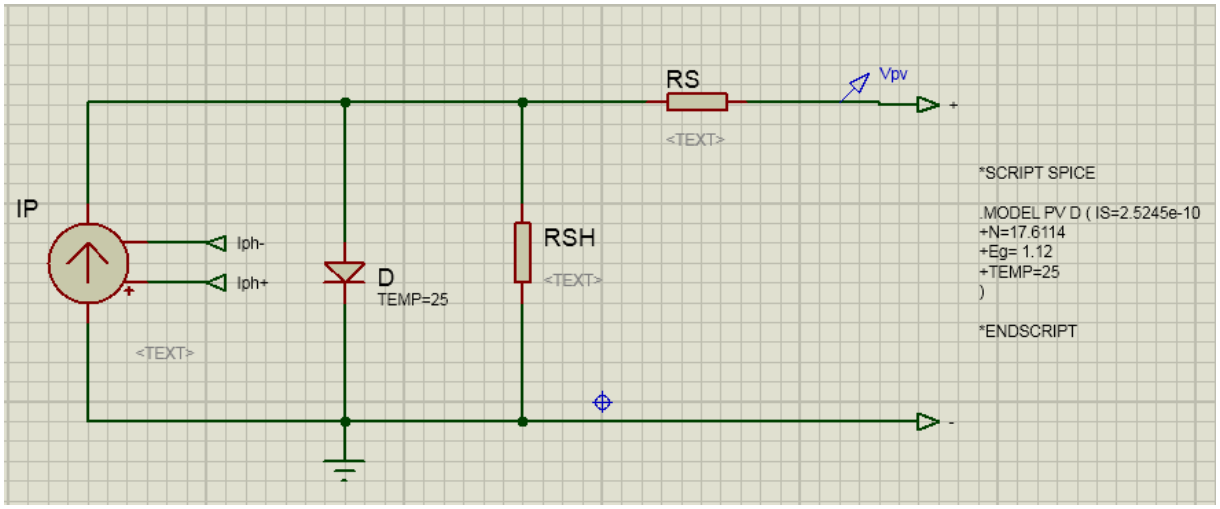

Figure IV.5: the PV panel model under Proteus.

As shown in Figure (IV.5), in order to model a PV panel in Proteus tool, the below steps are followed:

1. A “Voltage Controlled Current Source” block controlled by “DC Voltage Source” block is used to model the Current Source. For example, to simulate our model under STC, the value of “DC Voltage Source” block is set to 1.6216 V value, which is the photocurrent of P-5W panel under STC.

2. As shown in figure (IV.1), a diode with modified spice code is used in this model, because it is required to change the values of the saturation current Is, the ideality factor, number of cells and band gap energy in the Spice code according to the specification of P-5Welion panel [14]. Note that N is set to 17.6114 which is the multiplication between the ideality factor and number of cells.

3. Two resistors are used to model the shunt resistor and the series resistor with the values mentioned in table IV.1.

4. A “DC Voltage Source” block is connected to the PV panel model as a variable load. Its value is equal to the “Sweep variable” value of the “DC SWEEP ANALYSIS” graph used in order to simulate our model as shown in figure (IV.6), note that the range of “Sweep variable” variable must be between 0V and the open-circuit voltage. The simulation of the PV panel in ISIS Proteus is presented in Figure (IV.6).

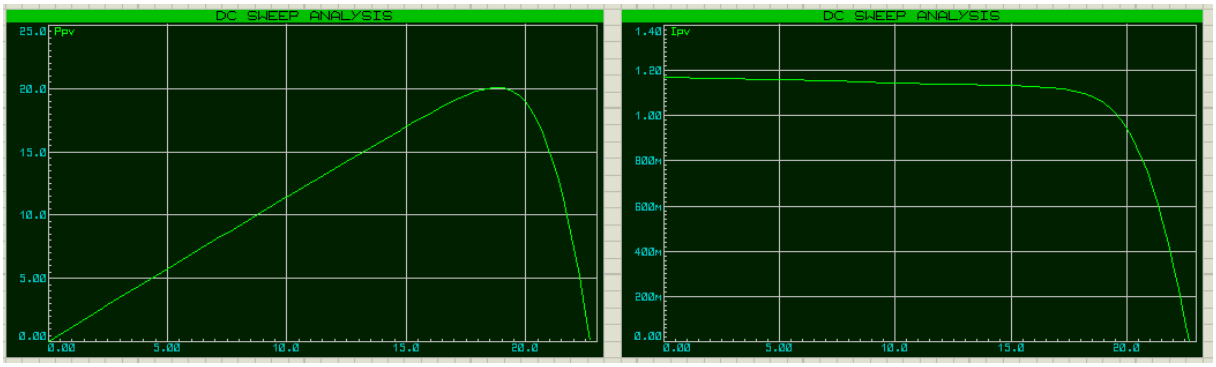

Figure IV.6: I-V and P-V characteristics for PV panel by using Proteus.

As presented in figure (IV.7), the Proteus PV model is put in a sub-circuit in order to make it easy to use.

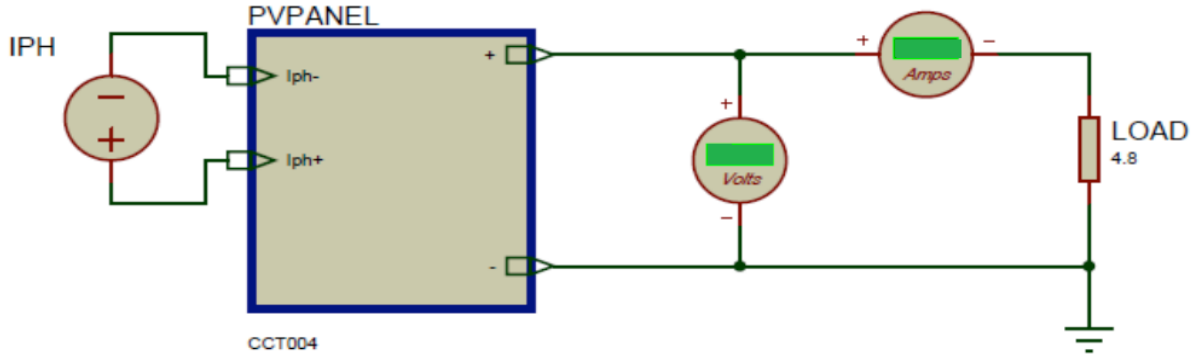

Figure IV.7: The sub circuit of the PV panel model under Proteus.

Modeling a PV panel in Proteus tool allows controlling our PV system by microcontroller and microprocessor. Therefore, the performance obtained will be similar to the performance obtained during real experience. One of the aims of this study is to acquire and supervise the current, voltage and power of our PV panel by using Arduino and Proteus.

IV.3 PV System Simulation under Proteus:

The simulation of the PV system under Proteus is shown in figure (IV.8).

The simulation results show that the DC-DC converter and the MPPT control perform their roles correctly. The inverter provides under optimal conditions a higher voltage at its output than the one provided by the PV generator.

The MPPT control adapts the PV generator to the load by transferring the maxi mum power The MPPT control adapts the PV array to the load by transferring the maximum power supplied by the PV array.

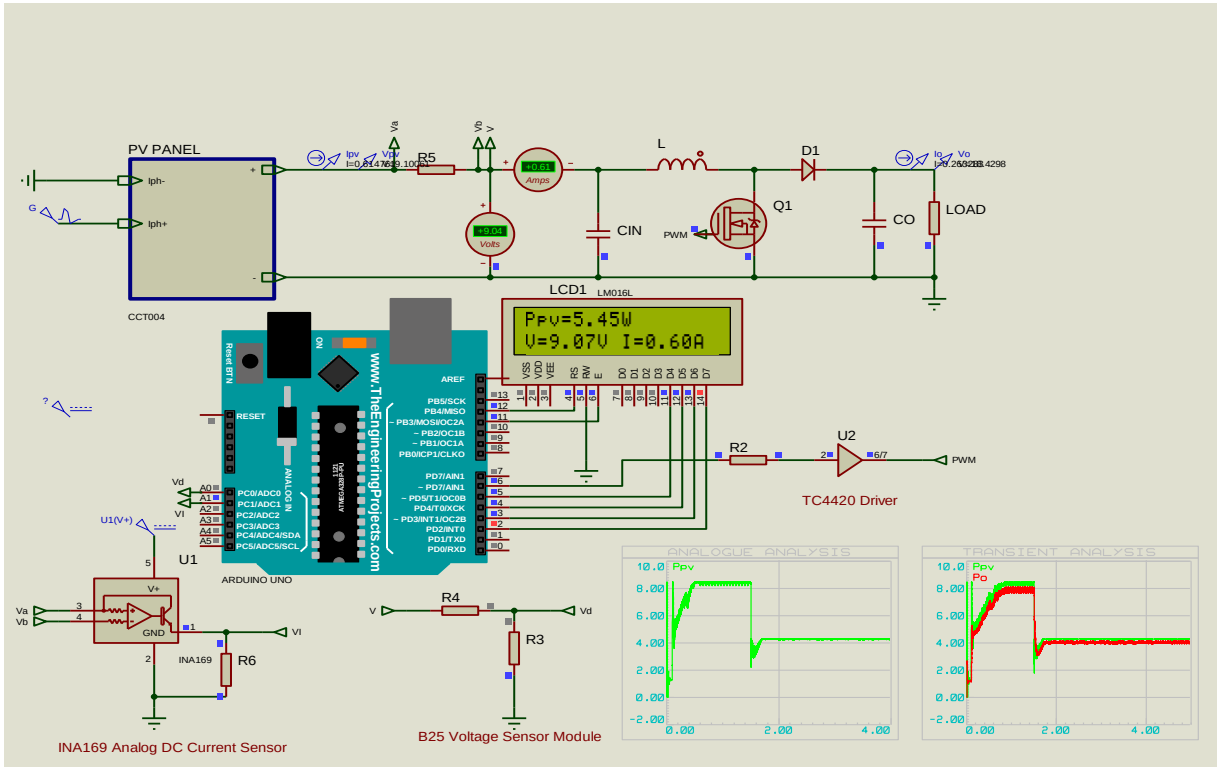

Figure (IV.8): Overall diagram of the photovoltaic system in Proteus.

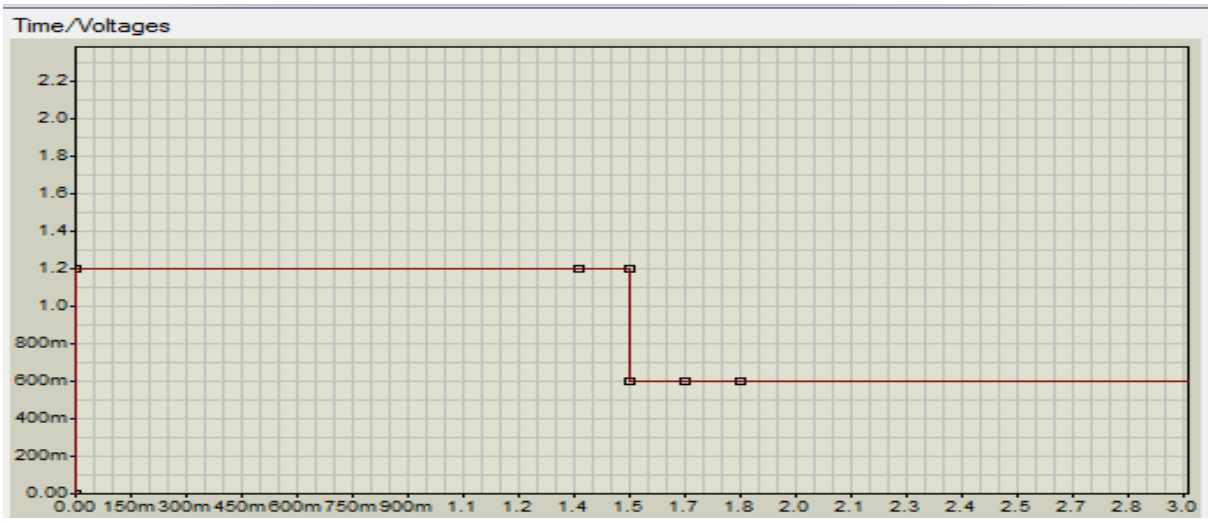

Figure (IV.9): changing in the solar radiation. Irradiance(W\m^2)

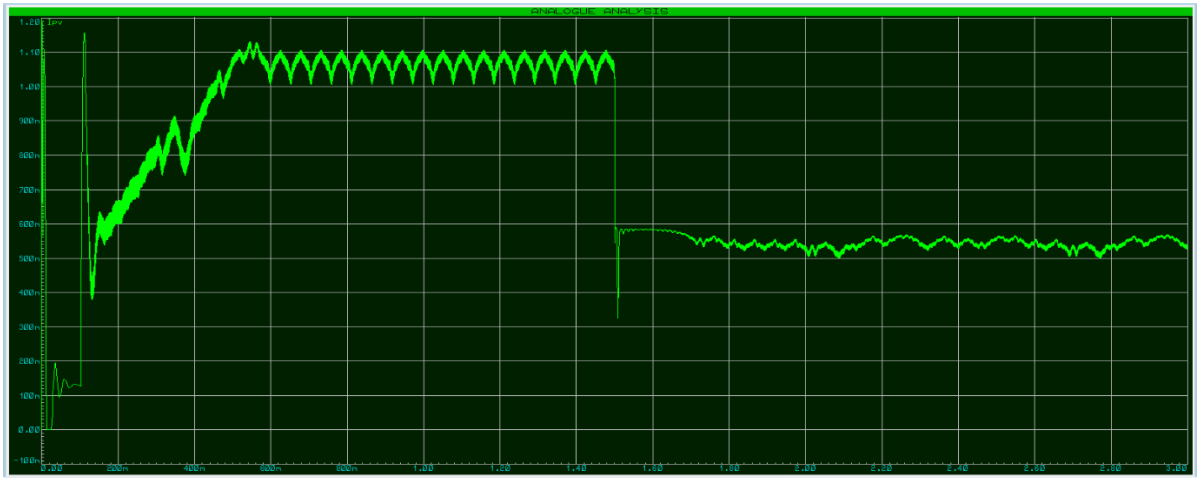

Figure (IV.10): maximized pic of the simulation results (Ipv).)
Current (A)

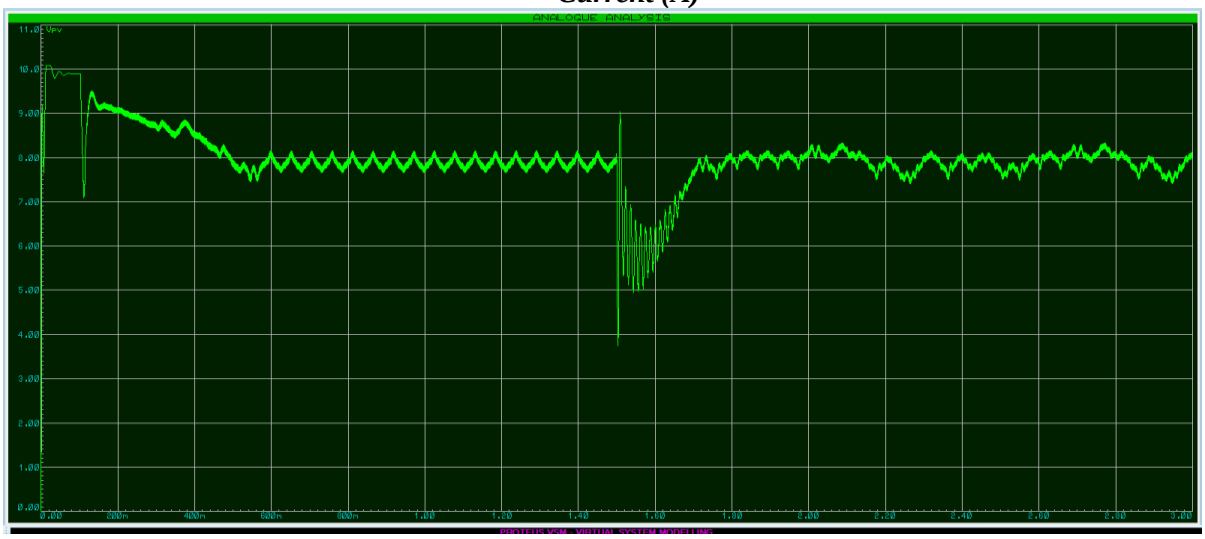

***Figure (IV.11): maximized* pic of the simulation results (Vpv) . Voltage(A)**

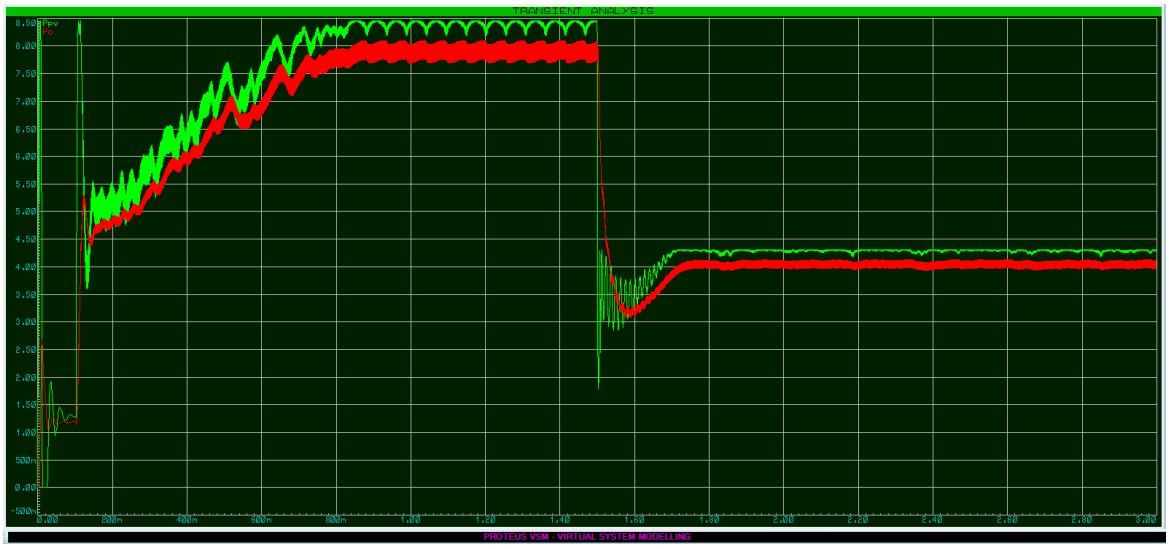

Figure (IV.12): maximized pic of the simulation results (comparing Ppv with Po).Powe(W)

Figure (IV.9) shows the Radiation profile used in simulation. Q=1.5s step change in radiation is applied to study the response of each technique during disturbance.

Figures (IV.10), (IV.11) shows the PV panel voltage and current while figure (IV.12) represents the comparison between the PV panel and the load power however, we notice that the pv power after rising suddenly it remains unchanged just till the perturbation is applied, the power fall for 2.5 watts peak and then made a significant recovery to stabilize and remain constant in its permanent range. At the same time, the load power trying to fellow the maximum power while the irradiation disturbance is applied in order to reach the highest level of power occurred by the solar panel and performs the correct decision in duty cycle.

The table shows the simulation results of the curves:

Table IV.2: the variation of power versus irradiance.

Irradiance	I_{PV}(A)	V_{PV} (V)	P_{PV} (W)	I_o(A)	V_o(V)	P_o(W)
200	0.4	4	1.6	0.47	2.8	1.316
600	0.62	6	3.72	0.70	5.7	3.99
1000	0.89	10	8.9	0.97	11.8	11.44

- Remarks and interpretations:

It appears that with different levels of illumination, the electrical quantities (power, voltage and current) stabilize around precise values.

the MPPT control makes the operating point oscillate around the MPP.

For a maximum irradiance E=1000 W/m2 the power supplied by the PV generator stabilizes around 8.9W and the power supplied to the load around 7.378W, at the output of the at the panel level, the voltage and current stabilize around 10V and 0.89A respectively.

At the load level, the voltage and current stabilize around 11.8 V and 0.97 A respectively.

IV.4 Characterization of the pv system:

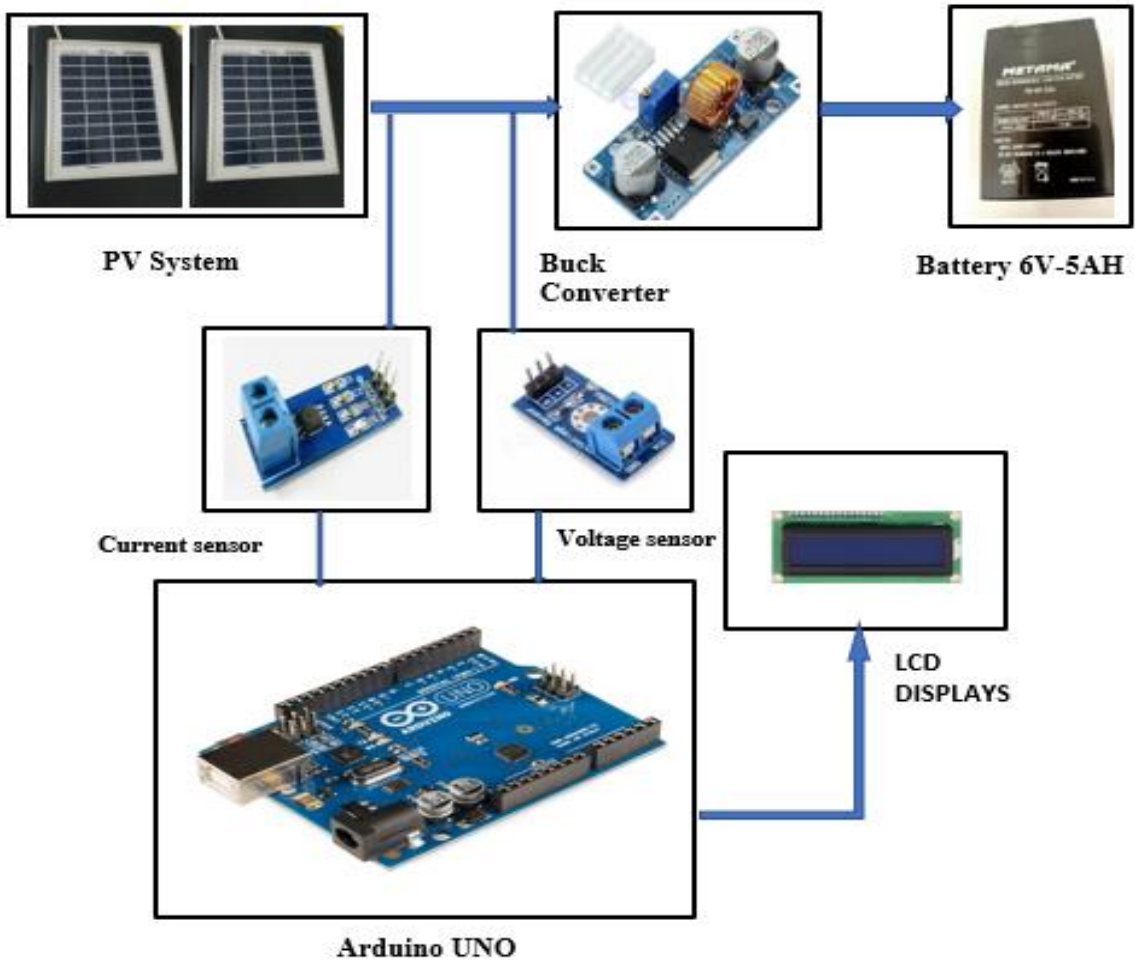

Figure IV.13: synoptic diagram of an MPPT controller.

IV.5 Hardware used:

IV.5.1 The microcontroller: [24]

The Arduino UNO board is a programmable ATmega328 microcontroller that can be used to operate components (motor, LED, etc.). It has "ports" allowing it to be connected to a computer or to be powered, for example. The Arduino UNO board is the centerpiece of any electronic circuit for beginners.

Figure IV.14 : La carte Arduino UNO.

IV.5.2 The software interface*:*

The Arduino IDE interface is rather simple (see Figure 4.2), it offers a minimal and uncluttered interface for developing a program on Arduino boards. It has a code editor with syntax highlighting (1) and a quick toolbar (2). These are the two most important elements of the interface, and are the ones we use most often.

There is also a more traditional menu bar (3) which is used to access the advanced functions of the IDE. Finally, there is a console (4) which displays the results of the compilation of the source code, operations on the board, etc

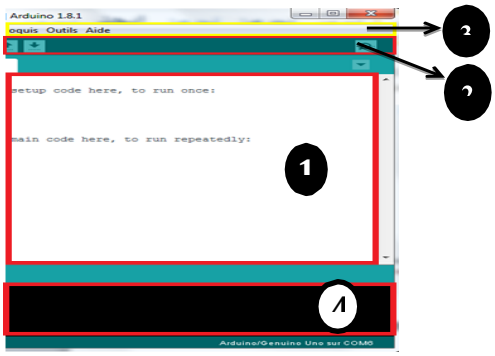

Figure IV.15: The Arduino IDE interface.

IV.5.3 Buck converter: [25]

The sizing of the Buck converter depends on the constraints imposed by the solar panel and the load.

Figure IV.16: Buck converter.

IV.5.4 Current sensor: [25]

The ACS712s sensor, this sensor is based on Hall Effect to measure AC or DC current signals accurately. The maximum current that can be supported by this module is 30A. The current signal present can be read out via analogue port.

Figure IV.17: Current sensor ACS712s.

IV.5.5 voltage sensor: [25]

3 pin voltage sensors (VCC, GND, and SIGnal) Can support up to 25V. This module is based on the principle of Pressure point resistance and it can make the input power voltage of the red terminal reduce 5 times of initial Voltage.

Figure IV.18 : Voltage sensor.

IV.5.6 The Solar panel:

We used the 11.6V, 5W, 0.62 A solar panel shown in figure (4.9)

FigureIV.19: Actual photo of used panel.

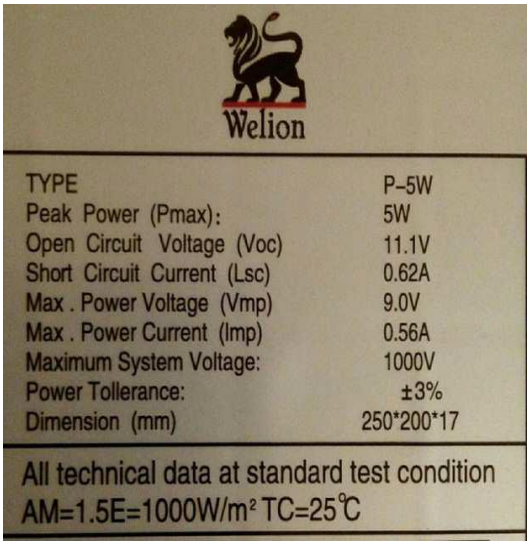

FigureIV.20: Used panel characteristics.

IV.5.7 LCD displays:

LCD displays have become indispensable in technical systems that require the display of the display of operating parameters.

These displays can show letters, numbers and some special characters.

The characters are predefined.

Figure IV.21: LCD displays.

IV.5.8 Battery:

A source of electric power consisting of one or more electrochemical cells with external connections for powering electrical devices.

Figure IV.22: METAMA battery 6V-5AH.

IV.6 Implementation with MPPT control:

The Maximum Power Point Tracking (MPPT) algorithm has been implemented in the Arduino. The IPV and VPV signals are filtered and then multiplied to obtain the value of the Average Power.

The details of the P&O based program are described in Appendix 2.

IV.6.1 Complete system assembly:

Made the complete assembly figure (IV.23). It is composed of a PV panel P-5W, buck converter, Arduino, current sensor (ACS712)30A, voltage sensor 25V and a battery 6V.

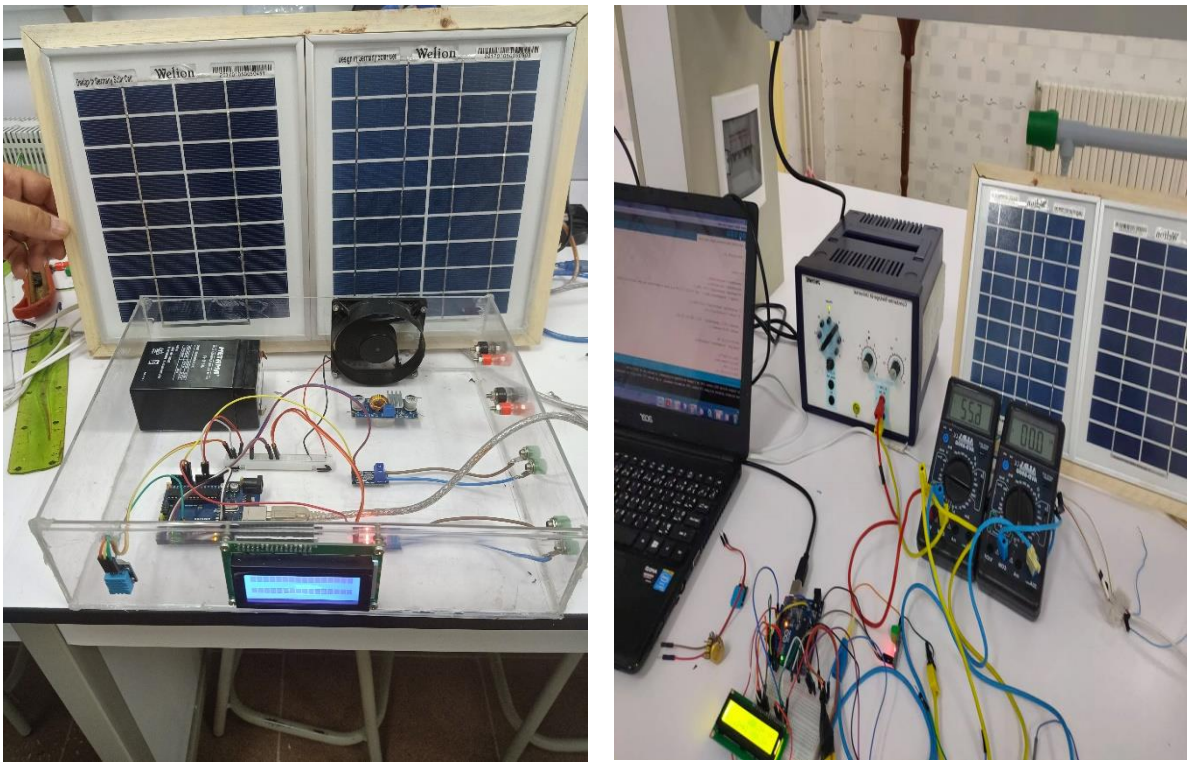

Figure IV.23: hardware prototype.

IV.6.2 Experimental results of the set-up:

Our objective is to change the irradiation as well as to find the PPM for each irradiance.

The values of the voltages, currents, powers and duty cycle remain varied around the values shown in the table IV.3 which we got from the LCD display figure IV.24:

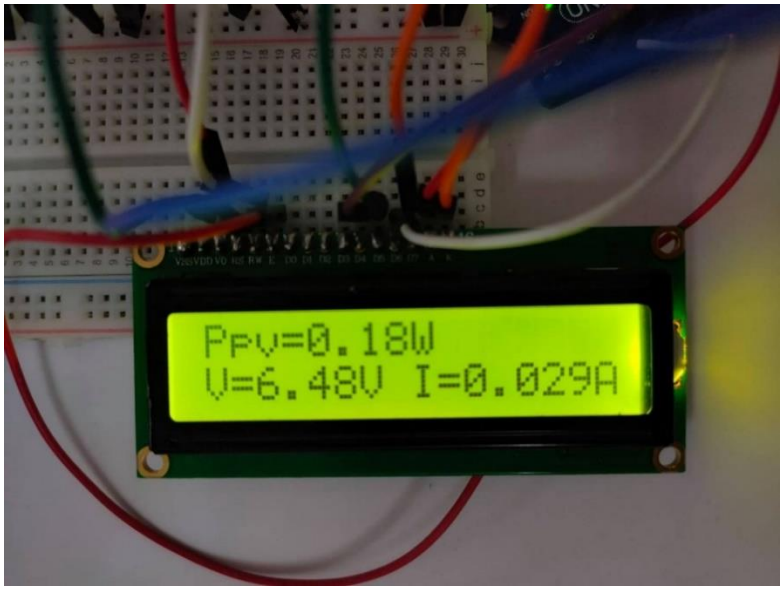

Figure IV.24:LCD display.

Table IV.3: Testing results of a P&O order.

Irradiation(W/m²)	*V_{pv}(V)*	*I_{pv} (A)*	*P_{pv}(W)*	*V_o(V)*	*Io (A)*	*P_o(W)*	*DC %*
200	*4*	*0.4*	*1.6*	*2.8*	*0.47*	*1.316*	*93*
600	*6*	*0.62*	*3.72*	*5.7*	*0.70*	*3.99*	*87*
1000	*10*	*0.89*	*8.9*	*11.8*	*0.97*	*11.44*	*90*

IV.6.3 Remarks and interpretations:

The results are in good agreement with the optimal ones deduced by the optimal analysis of the electrical quantities of the photovoltaic module. As a result, the realized photovoltaic system oscillates well around the maximum power point. In order to ensure a good functioning of the realized system and to estimate the power losses supplied by the photovoltaic module, we have characterized the realized system on irradiation variations:

- A good agreement between the experiment and the simulation of the previous chapter.
- The algorithm used ensures that the maximum power point is followed, without the photovoltaic system diverging. Despite the rapid variations in irradiation.
- The overall results obtained show that the PV system implemented works well.
- The Arduino and the algorithm used ensure optimal operation independently of irradiation variations. During this test.

IV.7 Comparison between simulation results and implementation:

Table IV.4 : Comparison of results between simulation and MPPT implementation.

	Measures				*Simulation*			
Ir(W/m2)	*Vpv(v)*	*Ipv(A)*	*Ppv(w)*	*Po(w)*	*Vpv(v)*	*Ipv(A)*	*Ppv(w)*	*Po(w)*
200	*7.5*	*0.6*	*6.2*	*7.412*	*4*	*0.4*	*1.6*	*1.316*
600	*7.67*	*0.92*	*9.80*	*9.49*	*6*	*0.62*	*3.72*	*3.99*
1000	*10.2*	*1.2*	*12.9*	*17.17*	*10*	*0.89*	*8.9*	*11.44*

By comparing with the measurements and the simulations, it can be concluded that the operation of the MPPT device and the whole test system is correct with losses up to 8.30watts.

IV.8 Conclusion:

The power losses in the conversion chain are negligible compared to the electrical power taken from the solar panel.

electrical power taken from the solar panel. The electrical power supplied to the battery will therefore be approximately equal to the power generated by the GPV. With an MPPT control, the PV generator can operate on its optimum electrical power curve over the entire range of irradiation and temperature variation.

General Conclusion

General conclusion:

The work presented is concerned with the analysis, modelling and simulation of the electrical electrical operation of a photovoltaic system with a digital control (MPPT control) for tracking the maximum power of the photovoltaic (PV) panels. In a first step, the PV systems, the principles of PV conversion and the technical characteristics of PV cells. In a second step, we analyzed the techniques of MPP tracking for the extraction of the maximum power under different operating conditions, known as the MPPT technique based on the based on the algorithms of inductance incrementing, perturbation and observation and Hill climbing algorithms followed by a comparison of the three algorithms in terms of accuracy and stability. Our judgment is that the Perturb and observe technique is the most suitable as it is easier to program and has an acceptable speed for our application.

Then we described in more detail the operation of the DC-DC because they are the main component of the photovoltaic system.

The role of a DC-DC converter with integrated MPPT plays the role of an automatic impedance matching of the load to ensure maximum power transfer.

In our work, we used a buck converter with MPPT with a control following the Perturb and observe algorithm installed on an Arduino Uno board. The buck converter was chosen because this type of converter has the best efficiency compared to other types, and that the open circuit PV voltage is11.1Vand the voltage at the maximum power point is 9V, which means that the source voltage is always higher than the voltage required by the load (a 6V battery).

By simulating the converter with the Proteus software, we were able to determine by trial and error the values of the components, in particular the resistors, the capacities and the inductance for the best possible performance.

At the end of the simulation we had built the prototype buck converter with MPPT.

The prototype was then subjected to various tests and measurements to fine-tune it by varying the radiation. The results obtained are satisfactory despite the relatively low power output.

The placement of a heat sink had reduced the heating of the battery.

In perspective, we admit that the prototype can be further improved by increasing the power conversion by adding more powerful components with heat sinks to protect them.

References

[1] Desideri, U., Zapparelli, F., & Garroni, E. (2013). Comparative analysis of concentrating solar power and photovoltaic technologies: Technical and environmental evaluations. Science Direct, 765-784. e

[2] R. D. Middlebrook, Power electronics: topologies, modeling, and measurement, Proc. IEEE Int. Symp. Circuits Syst., April 1981.

[3] R. Severns and G. E. Bloom, Modern Dc-to-Dc Switchmode Power Converter Circuits, New York: Van Nostrand Reinhold, 1985.

[4] J. van der Heide, in Comprehensive Renewable Energy, 2012

[5] D.M. Chapin, C.S. Fuller, G.L. Pearson, Journal of Applied Physics 25 (1954) 676

[6] C. Julian Chen. Physics of Solar Energy, 1st ed. Hoboken, NJ, USA: John Wiley & Sons Inc., 2011.

[7] G. Boyle. Renewable Energy: Power for a Sustainable Future, 2nd ed. Oxford, University Press, 2004.

[8] Yuncong Jiang and Jaber A. Abu Qahouq, "Evaluation of Output Current PV MPPT Controller with Different Step Sizes and Multiple Panels or Cells", Twenty-Seventh Annual IEEE Applied Power Electronics conference and Exposition (APEC), 2012, pp. 1872-1876.

[9] Vincheh, M. R., Kargar, A., & Markadeh, G. A. (2014). A hybrid control method for maximum power point tracking (MPPT) in photovoltaic systems. Arabian Journal for Science and Engineering, 39(6), 4715-4725.

[10] Singh, P., Singh, S. N., Lal, M., & Husain, M. (2008). Temperature dependence of I–Vcharacteristics and performance parameters of silicon solar cell. Solar Energy Materials and Solar Cells, 92(12), 1611-1616.

[11] R.P. Mukund, « Wind and solar Power Systems », Ph.D., P.e U. S merchant Marine Academy, Kings Point, New York, CRC Press LLC 1999.

[12] C. R. Sullivan and M. J. Powers, « High-efficiency maximum power

[13] point tracker for photovoltaic arrays in a solar-powered race vehicle » The 1993 IEEE 24th Annual Power Electronics Specialists Conference, PESC Record, pp 574-580, Seattle, WA, USA, 1993.

[14] E. Carroll, High power active devices, CAS Power Converters for Particle Accelerators, Warrington, 2004

[15] A.W. Kelley and W.F. Yadusky, Rectifier design for minimum line-current harmonics and maximum power factor, IEEE Trans. Power Electron. 7 (1992) 332.

[16] P Proudlock, Achieving. high performance, CAS – Power Converters for Particle Accelerators, Montreux, 1990 (CERN 90-07).

[17] Cabal, C. Energy optimization of the electronic matching stage dedicated to photovoltaic conversion(Doctoral dissertation, University of Toulouse, University Toulouse (2008).

[18] YAAKOUB BENYAHIA "Modeling and simulation of a photovoltaic system adapted by a MPPT control" Oum El Bouaghi-2013

[19] Nicola Femia, Giovanni Petrone, Giovanni Spagnuolo and Massimo Vitelli, "Optimization of Perturb and Observe Maximum Power Point Tracking Method" IEEE Transactions on Power Electronics, Vol. 20, No. 4, July 2005, pp. 963-973.

[20] Ashraf Ahmed, Li Ran and Jim Bumby, "Perturbation Parameters Design for Hill Climbing MPPT Techniques" IEEE International Symposium on Industrial Electronics(ISIE), 2012, pp. 1819-1824,

[21] Hamdy Radwan and Mohamed Orabi, "The Non Ideality Effect of Optimizing the P&O MPPT Algorithm for PV Stand-Alone Applications", IEEE 34th International Telecommunications Energy Conference (INTELEC), 2012, pp. 1 – 7.

[22] D. P. Hohm, M. E. Ropp, "Comparative Study of Maximum Power Point Tracking Algorithms Using an Experimental, Programmable, Maximum Power Point Tracking Test Bed" Conference Record of the Twenty-Eighth IEEE Photovoltaic Specialists Conference, pp: 1699 – 1702, 2000.

[23] Mohammed A. Elgendy, Bashar Zahawi and David Atkinson, " Assessment 0f P&O MPPT Algorithm Implementation Techniques for PV Pumping Applications", IEEE Transactions on Sustainable Energy, Vol. No. 1, January 2012, pp. 21-33.

[24] Yongheng Yang and Frede Blaabjerg, "A Modified P&O MPPT Algorithm for Single Phase PV Systems Based on Deadbeat Control", 6th IET International Conference on Power Electronics, Machines and Drives (PEMD), 2012, pp.1-5.

[25] J H R Enslin, "Power Point Tracking: A Cost Saving Necessity in Solar Energy Systems" 16th Annual Conference of IEEE Industrial Electronics Society, vol.2, pp. 1073 – 1077, 1990.

Drypower

VRLA AGM MULTIPURPOSE RANGE

BACKUP & MAIN POWER

6V | 5Ah | SLA | AGM

6SB5P

Rechargeable AGM Sealed Lead Acid Battery

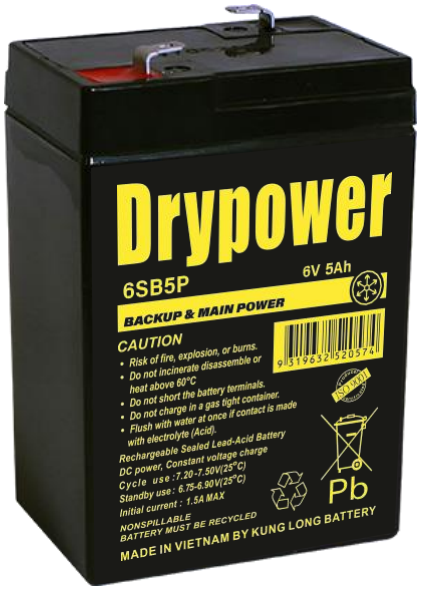

SPECIFICATIONS

Nominal Voltage		6V
Nominal Capacity		
20 hour rate	(0.250A to	5Ah
10 hour rate	(0.428A to	4.275Ah
5 hour rate	(0.765A to	3.825Ah
1C	(4.5A to	2.55Ah
3C	(13.5A to	1.80Ah
Weight		Approx. 820g
Internal Resistance (at 1KHz)		Approx. 19mΩ
Maximum Discharge Current (5		67.5A
Charge Methods at 25°C		
Cycle Use		7.20V to 7.50V
Charging	Coefficient	1.35A
Maximum Charging		6.75V to 6.90V
Standby Use		
Float Charging	Coefficient	-3.0mV/°C/Cell
Charge		
Discharge		–15°C to
Storage		–15°C to
Charge Retention (Shelf Life) at 20°C		
1 month		92%
3 months		90%
6 months		80%
Case Material		ABS UL94 HB
Design Life		3-5 Years
Termination		F1 (Faston

Classified as a non-spillable battery.
Approved for transportation by:
- Air (IATA/ICAO
- Sea (per IMDG Special

IATA

9319632520574

DIMENSIONS mm (inch)

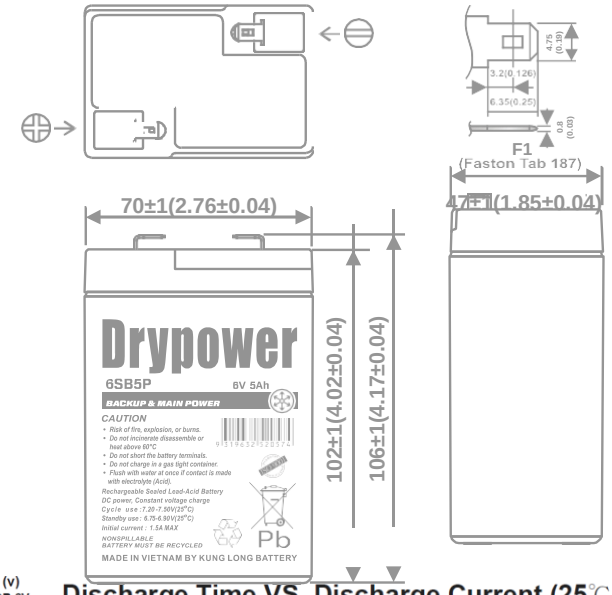

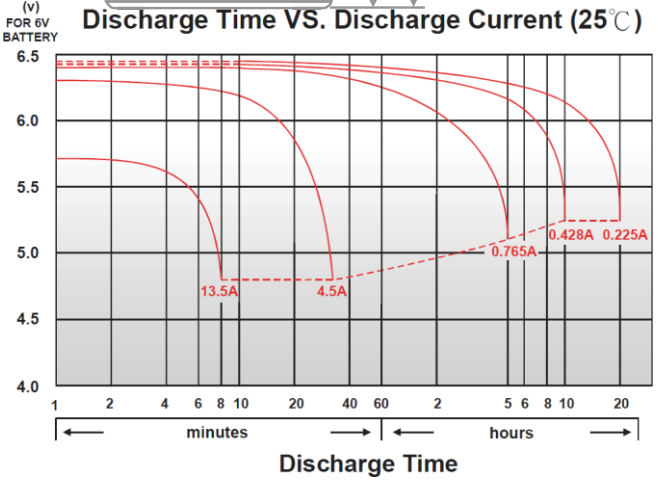

Drypower

6SB5P (6V 5Ah)

CHARACTERISTICS CHARTS

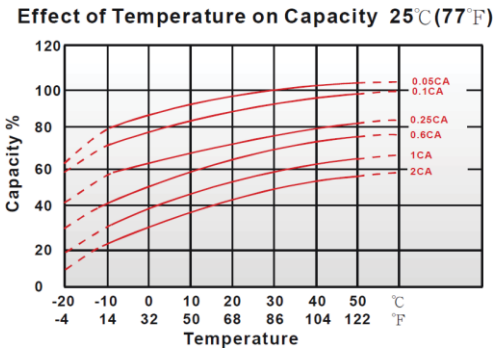

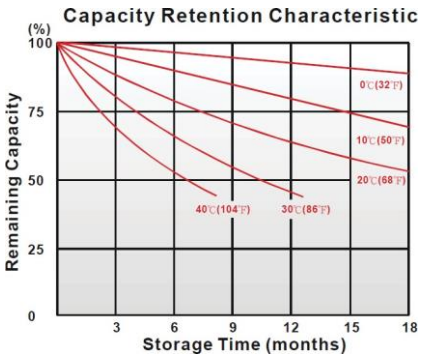

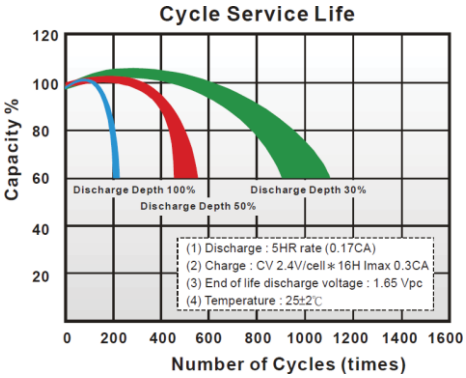

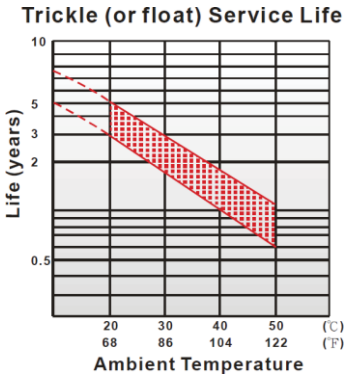

FEATURES & BENEFITS

- Industry leading 99.99% pure lead content for superior service life and dependable performance.
- Maintenance free technology and non-spillable design.
- Excellent charge retention in storage.
- Higher percentage of tin content compared with the industry standard. Tin extends battery standby life by minimising sulphation (corrosion) especially at higher temperatures.
- Manufactured by Kung Long Battery (KLB) at facilities in Taiwan and Vietnam.

  KLB is a leading manufacturer and complies with relevant international quality standards including ISO9001, CE ETL9000, UL1989, OHSAS18001 and ISO17025.

  KLB supports Green Sustainable supply chain practices.

PERFORMANCE DATA

Discharge Rates in Watts to Various End Voltages at 25°C (77°F)

Time \ End Voltage		1.85V	1.80V	1.75V	1.70V	1.67V	1.65V	1.60V
5	min	23.8	26.8	29	31	31.8	32.8	34
10	min	17	19.2	20.5	21.5	22	22.5	23
15	min	14.1	15.6	16.2	16.5	16.7	16.8	17
30	min	8.18	9.15	9.52	9.7	9.8	9.92	10
60	min	4.2	4.77	5.13	5.43	5.53	5.65	5.73
120	min	2.48	2.77	2.9	3	3.05	3.12	3.18
180	min	1.97	2.17	2.27	2.35	2.38	2.43	2.48
240	min	1.6	1.73	1.8	1.85	1.88	1.92	1.95
300	min	1.46	1.56	1.6	1.64	1.65	1.68	1.72
600	min	0.855	0.913	0.94	0.96	0.97	0.978	0.992
1200	min	0.432	0.468	0.498	0.51	0.513	0.52	0.527

Discharge Rates in Amperes to Various End Voltages at 25°C (77°F)

Time \ End Voltage		1.85V	1.80V	1.75V	1.70V	1.67V	1.65V	1.60V
5	min	15.3	17.6	18.9	19.5	19.7	19.9	20.2
10	min	10.5	11.7	11.9	12.1	12.2	12.3	12.4
15	min	7.56	8.22	8.71	8.92	8.99	9.07	9.15
30	min	4.39	4.94	5.11	5.25	5.3	5.35	5.41
60	min	2.36	2.61	2.73	2.84	2.87	2.91	2.94
120	min	1.32	1.44	1.5	1.54	1.55	1.57	1.59
180	min	1.09	1.15	1.18	1.2	1.21	1.22	1.23
240	min	0.84	0.891	0.916	0.942	0.948	0.955	0.963
300	min	0.776	0.812	0.825	0.837	0.841	0.846	0.852
600	min	0.435	0.452	0.464	0.473	0.477	0.481	0.486
1200	min	0.219	0.233	0.241	0.247	0.25	0.253	0.257

All data on the spec. sheet is an average value:

The tolerance range : X < 6min (+15%~–15%), 6min ≤ X < 10min (+12%~–12%), 10min ≤ X < 60min (+8%~–8%), X ≥ 60min (+5%~–5%)

Aug2020

Appendix 2:

```
int duty = 75;
const int v = A0;
const int I = A1;
int vk = 0;
int ik = 0;
int p = 0;
int delP = 0;
int vprev = 0;
int p_prev = 0;
int delv = 0;
const int wave = 5;

void setup () {pinMode (wave, OUTPUT);}
void loop () {
// put your main code here, to run repeatedly:
 vk = analogRead(v);
 ik = analogRead(I);
  vk= (5/1023) *vk; //analog read will give value between 0 to 1023.
 ik= (5/1023) *ik;
 p = vk*ik;
delP = p - p_prev;
delv = vk-vprev;
if (delP! =0 || delv! =0)
{
  if (delP > 0) {
    if (delv < 0) {
     duty++;
    }else{
      duty--;
    }
 } else {
    if (delv<0) {
     duty--;
    } else {
     duty++;
    }
  }
}
else {
  duty = duty;
  } digital Write (wave, HIGH);
 delay Microseconds(duty);
 digital Write (wave, LOW);
 delay Microseconds(100-duty);
   p_prev=p;
   vprev=vk;
      }
```